# Process studies at the air-sea interface after atmospheric deposition in the Mediterranean Sea: objectives and strategy of the PEACETIME oceanographic campaign (May-June 2017)

Cécile Guieu[1], Fabrizio D'Ortenzio[1], François Dulac[2], Vincent Taillandier[1], Andrea Doglioli[3], Anne Petrenko[3], Stéphanie Barrillon[3], Marc Mallet[4], Pierre Nabat[4], Karine Desboeufs[5]

[1] CNRS, Sorbonne Université, Laboratoire d'Océanographie de Villefranche, UMR7093, Villefranche-sur-Mer, France

[2] Laboratoire des Sciences du Climat et de l'Environnement (LSCE), UMR 8212, CEA-CNRS-UVSQ, IPSL, Univ. Paris-Saclay, CEA Saclay, Gif-sur-Yvette

[3] Aix-Marseille Université, CNRS, Université de Toulon, IRD, Mediterranean Institute of Oceanography, UMR 7294, Marseille, France

4 Centre National de Recherches Météorologiques, Météo-France/CNRM/GMGEC/MOSCA, Toulouse, France

[5] LISA (Laboratoire Interuniversitaire des Systèmes Atmosphériques), UMR CNRS 7583, Université de Paris, Université Paris Est, IPSL, Créteil, France

## Abstract

In spring, the Mediterranean Sea, a well-stratified low nutrient low chlorophyll region, receives atmospheric deposition ~~both~~ desert dust from the Sahara and airborne particles from anthropogenic sources. Such deposition ~~translates into a~~ supply of new nutrients and trace metals ~~for~~ the surface waters that likely impact biogeochemical cycles. However, ~~the~~ quantification of ~~the~~ impacts and ~~the~~ processes involved ~~are still~~ far from being ~~assessed in situ~~. ~~In this paper,~~ we provide ~~a state of the art regarding~~ dust deposition and its impact on the Mediterranean Sea biogeochemistry and ~~we~~ describe in this context the objectives and strategy

of the PEACETIME project and cruise, entirely dedicated to filling this knowledge gap. Our strategy to ~~go a step forward than in previous approaches in~~ understanding these impacts by ~~catching~~ a real deposition event at sea is detailed. The PEACETIME oceanographic campaign took place in May-June 2017 and ~~we describe how we were~~ able to successfully adapt the planned transect ~~in order~~ to sample a Saharan dust deposition event~~, thanks to a dedicated strategy,~~ so-called 'Fast Action'. ~~That was successful, providing,~~ for the first time ~~in~~ our knowledge, a coupled atmospheric and oceanographic sampling ~~before,~~ during and after an atmospheric deposition event. Atmospheric and marine in situ observations and process studies ~~have been~~ conducted in contrasted area ~~and we summarize~~ the work performed at sea, the ~~type of~~ data acquired and their ~~valorization in the papers published~~ in ~~the~~ special issue.

## 1. Introduction

Understanding the exchange of energy, gases and particles at the ocean–atmosphere interface is critical for the development of robust predictions of future climate change and its consequences on marine ecosystems and the services they provide to society. Our understanding of such exchanges has advanced rapidly over the past decade but we remain unable to adequately parameterize fundamental controlling processes as identified in the new research strategies of the international Surface Ocean–Lower Atmosphere Study group (Law et al., 2013 and SOLAS 2015-2025: Science Plan and Organisation). A critical bottleneck is the parameterization and representation of the key processes brought into play by atmospheric deposition in Low Nutrient Low Chlorophyll (LNLC) regions. A perfect example of a LNLC region, and of the role of the atmospheric deposition, is the Mediterranean Sea where the ecosystem functioning may be modulated by pulsed atmospheric inputs in particular the deposition of Saharan dust (Guieu et al., 2014a) and nutrients of anthropogenic origin (Richon et al., 2018a, 2018b).

Indeed, the Mediterranean quasi-enclosed basin continuously receives anthropogenic aerosols originating from industrial and domestic activities from all around the basin and other parts of Europe, both in the western (Bergametti et al., 1989; Desboeufs et al., 2018) and eastern (Tsapakis et al., 2006; Moon et al., 2016) basin. In addition to this continuous 'background' inputs, the surface of the Mediterranean Sea episodically receives biomass burning particles (Guieu et al., 2005) and Saharan dust (e.g. Loÿe-Pilot et al., 1986, Vincent et al., 2016). Some deposition events are qualified as 'extreme events', as dust inputs as high as 22 g $m^{-2}$ (event in Nov. 2001 recorded at Ostriconi-Corsica Island, Guieu et al., 2010; event in Feb. 2002 recorded at Cap Ferrat, Bonnet and Guieu, 2006) can occur on very short time scales (hours to days) ~~representing the main~~ annual dust flux. Associated atmospheric deposition of major macro-nutrient (N, P) (Kouvarakis et al., 2001; Markaki et al., 2003, 2010; Guieu et al., 2010), ~~of~~ iron (Bonnet and Guieu, 2006) and ~~of~~ trace metals (Theodesi et al., 2010; Guieu et al., 2010; Desboeufs et al., 2018) represents significant inputs likely ~~supporting the~~ primary production in surface waters especially during ~~the stratification~~ period (Richon et al., 2018a, 2018b). Among the atmospheric deposited nutrients, anthropogenic reactive nitrogen is critical ~~on~~ the ~~fluxes of~~ inorganic and organic N (Markaki et al., 2010, Violaki et al., 2010). Soil dust deposition plays an important role ~~on the fluxes of~~ P and trace metals due to ~~the intense~~ but ~~sporadic inputs~~ (Bergametti et al., 1992; Guieu et al., 2010; Morales-Baquero and Perez-Martinez, 2016), ~~even if~~ the contribution of anthropogenic aerosol deposition is significant (between less ~~of~~ 10 % (Fe) and 90% (Zn)) (Guieu et al., 2010, Desboeufs et al., 2018). The atmospheric deposition of mineral dust is correlated with dissolved trace metals enrichment of the sea-surface microlayer (Cd, Co, Cu, Fe) (Tovar Sanchez et al., 2014). However, it has been shown that dust deposition can result either in a net release or in scavenging of dissolved inorganic phosphorus and nitrate (Louis et al., 2015) and trace elements in seawater (Wagener

et al., 2010; Wuttig et al., 2013; Bressac & Guieu 2013), depending on the quantity and quality of in situ dissolved organic matter at the time of the deposition.

Recent studies in pelagic large mesocosms ~~also allowing quantifying the export below~~, have shown that wet Saharan dust analog deposition, by providing P and N for marine biosphere, strongly stimulates primary production and phytoplanktonic biomass during several days (Ridame et al., 2014; Guieu et al., 2014b; Tsagaraki et al., 2017). In addition to being strongly stimulated by atmospheric P (Ridame et al., 2013), the trace metals in dust deposition have been also ~~suspected~~ to stimulate $N_2$ fixation in the Mediterranean Sea (Ridame et al., 2011). The extension of ~~this~~ fertilizing effect of dust events over the Mediterranean has been pointed out from ~~statistically positive~~ correlations between dust deposition and surface chlorophyll concentrations from remote sensing and modelling approaches (Gallisai et al., 2014). A negative effect of atmospheric deposition on chlorophyll is, however, observed in the regions ~~under~~ a large influence of aerosols from ~~European origin~~ (Gallisai et al., 2014). ~~Indeed,~~ the input of anthropogenic aerosols, ~~as~~ Cu~~-rich aerosol,~~ ~~has been suspected to~~ inhibit phytoplankton growth (Jordi et al., 2012). Besides phytoplankton, dust deposition ~~modifies~~ also ~~the~~ bacterial community structure by selectively stimulating and inhibiting ~~certain members of the bacterial~~ community (Pulido-Villena et al., 2014; Tsagarakis et al., 2017). The budgets established from 4 artificial seeding experiments during project DUNE (Guieu et al., 2014b) all showed that ~~stimulating predominantly heterotrophic bacteria,~~ atmospheric dust deposition can enhance the remineralization of dissolved organic carbon (DOC), thereby reducing net atmospheric $CO_2$ drawdown. This also reduces the fraction of DOC that ~~can be mixed and~~ exported to deep waters during ~~the~~ winter mixing (Pulido-Villena et al., 2008). Similarly, dust addition ~~using on-land~~ mesocosms in the eastern Mediterranean Sea suggested that ~~the~~ auto- and hetero-trophic components of the food web were enhanced by the ~~dust addition thanks to the~~ nitrogen and

phosphorus added through dust (Pitta et al., 2017 and companion papers) ~~and that~~ the response was independent of ~~the way the~~ dust was added to the surface waters ~~(~~single strong pulse or three repetitive smaller pulses~~)~~. One of the most intriguing results is the role of Saharan dust deposition in the export of particulate organic carbon (POC) to ~~the deep Mediterranean Sea~~ by both fertilizing and acting as ballast ~~and~~ facilitating aggregation ~~processes~~ (i.e. Ternon et al. 2010, Bressac et al., 2014; Desboeufs et al., 2014; Louis et al., 2017; Guieu et al., in prep.). Experimental ~~approaches~~ have shown that wet dust deposition ~~events, by supplying bioavailable new nutrients, presents~~ a higher positive impact compared to dry deposition, ~~on both~~ marine primary ~~production~~, nitrogen ~~fixation and chlorophyll concentration~~s (Ridame et al., 2014; Guieu et al., 2014b).

Over the past decade, most of these valuable findings have been made thanks to experimental approaches based on dust and aerosols addition in~~to~~ bottle~~s and~~ up to large in-situ mesocosm~~s or using~~ remote sensing approaches. In this paper, we provide a state of the art regarding dust deposition and its impact in the Mediterranean Sea and we describe our strategy to go a step forward by catching a real wet deposition event at sea in order to study in situ the effects of the rapid introduction of chemical elements and particles from the atmosphere onto the marine element cycles, the biology and the export of material to the deep waters.

## 2. PEACETIME objectives

In this context, the PEACETIME project (ProcEss studies at the Air-sEa Interface after dust deposition in the MEditerranean sea) (http://peacetime-project.org/; last access 9 Feb. 2020) aimed at extensively studying and parameterizing the chain of processes occurring in the Mediterranean Sea after atmospheric deposition, especially of Saharan dust, and ~~to put them in perspective of on-going environmental changes. The ultimate goal was to~~ assess how these

mechanisms impact, and will impact in the future, the functioning of the marine biogeochemical cycles, the pelagic ecosystem and the feedback to the atmosphere.

The PEACETIME project was centered on a one-month oceanographic cruise in the central and western Mediterranean Sea in May-June 2017. The strategy during the cruise was designed to tackle the following questions:

1. How does atmospheric deposition impact trace element distribution in the column ~~water~~ including the sea surface microlayer?
2. What is the role of dissolved organic matter~~/particulate~~ dynamics on the fate of deposited atmospheric trace elements?
3. How does atmospheric deposition impact biogeochemical processes and fluxes? Do in situ biogeochemical /physical conditions matter?
4. What is the impact of atmospheric deposition on biological activity and on the structure and composition of the planktonic communities?
5. How does atmospheric deposition impact the downward POC export and ~~the~~ subsequent carbon sequestration?
6. What is the impact of biogeochemical conditions on gases and aerosol emissions from the surface water?
7. How are optical properties above and below the air-sea interface impacted by aerosols emission and dust deposition?

During the 33 day cruise, 40 scientists from the atmosphere and ocean communities travelled 2750 nautical miles (4300 km) performing simultaneously in situ sampling in the lower atmosphere and the water column, and conducting on board experiments in climate reactors simulating present and future marine physical conditions. The impacts on the cycles of chemical elements, on marine biogeochemical processes and fluxes, on marine aerosols emission were

investigated in a variety of oligotrophic regimes. Characterizations of the chemical, biological, physical and optical properties of both the atmosphere and the sea-surface microlayer, mixed layer and deeper waters were ~~performed~~.

The time of the campaign and the adaptive strategy for the cruise track, based on the daily analysis of a number of operational forecast and near real-time observational products were designed to maximize the probability to ~~catch~~ a Saharan dust deposition event in a stratified water column in order to ~~follow in-situ~~ the associated processes. In this paper, we describe how our strategy was designed before the campaign and how we were able to adapt it during the cruise in order to sample a Saharan dust deposition event at sea, thanks to a dedicated and so-called Fast Action prompted during the cruise.

## 3. Best time to schedule PEACETIME cruise

~~154~~ In order to fulfil the objectives of the PEACETIME cruise, ~~the occurrence probability of a significant atmospheric deposition event was maximized by choosing to do~~ the cruise during a period of surface water stratification. ~~This criterium matters because~~ atmospheric inputs ~~can be the main external nutrient supply~~ to offshore surface waters ~~during the stratification period~~ (Guerzoni et al., 1999; The Mermex Group, 2011; Richon et al., 2018a). The Mediterranean surface mixed layer depth monthly climatology (figure 1) shows a basin scale deepening from November to February–March and an abrupt re-stratification in April, which is maintained throughout summer and early autumn (D'Ortenzio et al., 2005). With mixed layer depths ~~below~~ 30 m ~~in~~ the whole Mediterranean ~~basin~~, the May-September period ~~looks~~ particularly favorable to sample highly stratified waters, ~~with possible consideration of~~ April and October ~~months~~ (~~<~~40 m).

~~Because African dust transport associated to rain period generally leads to the highest atmospheric deposition fluxes in the Mediterranean region (e.g., Loÿe-Pilot et al., 1986; Kubilay et al., 2000; Fu et al., 2017), we checked the probability that a Saharan dust event may occur during the cruise~~. The satellite-derived monthly climatologies of dust in the atmospher~~ic~~ ~~column~~ over the Mediterranean show a maximum in summer in the western basin and ~~in~~ spring and summer in the central basin (e.g., Moulin et al., 1998; Varga et al., 2014). ~~Consistently, model results in Figure 2 shows the highest values of dust aerosol optical depth (>0.10 and up to 0.30 at 550 nm) over the whole western and central basins from May to August, an intermediate situation in April and September, and the lowest values (generally <0.10) from October to February~~. In addition to ~~this seasonality of~~ the dust ~~columnar~~ load, the climatology of $PM_{10}$ and associated African dust concentration at the surface in the Mediterranean indicates that the occurrence of dust plumes close to the surface, i.e. prone to dry deposition, is ~~maximum~~ in April-May in Greece, April-June in Sicily, May-June in continental Italy, May in SE France, June-July in NE Spain and July-August in SE Spain (Pey et al., 2013). From weekly insoluble deposition monitoring at 4 sites ~~of~~ western Mediterranean islands (Frioul, Corsica, Mallorca and Lampedusa) ~~in the period 2011-2013~~, Vincent et al. (2016) report that ~~most of~~ the most intense African dust deposition events occurred between March and June.

Literature from deposition measurements at various sites in the western Mediterranean highlights a spring maxima for dust deposition (Bergametti et al., 1989; Loÿe-Pilot and Martin, 1986; Avila et al., 1997; Ternon et al., 2010; Desboeufs et al., 2018). Moreover, observations indicate that the highest deposition fluxes of dust are most often associated with wet deposition episodes (e.g. Loÿe-Pilot et al., 1986; Bergametti et al., 1989; Guerzoni et al., 1995; Loÿe-Pilot and Martin, 1996; Avila et al., 1997; Kubilay et al., 2000, Dulac et al., 2004; Guieu et al., 2009; Ternon et al., 2010; Vincent et al., 2016). A survey of dust wet deposition events at Montseny

stations in NE Spain ~~over~~ 1996-2002 ~~concluded that the maximum~~ frequency ~~was~~ in May (about 3 events per month) ~~and~~ June and November (about 1 event per month). ~~Data from Vincent et al. (2016) also show that~~ most ~~of the two-three highest~~ dust deposition events ~~recorded at each of the 4 island stations cited above~~ occurred between March and May, and ~~are most~~ often associated with rainfall.

It was also important that the cruise crossed different trophic regimes to ~~get likely contrasted~~ responses to atmospheric deposition. Although the Mediterranean is classified as an oligotrophic basin characterized by low-nutrient concentrations, there is a general west-to-east gradient of increasing oligotrophy (The Mermex Group (2011) and references within). ~~Figure 3 shows monthly averaged satellite-derived Chl-a concentrations in the Mediterranean basin :~~ from April to June, various trophic conditions can be found in the basin, with still relatively "high" Chl-a concentrations (0.3 mg $m^{-3}$) in the Ligurian and Alboran Sea and ultra-oligotrophic conditions in the central and eastern basin (< 0.03 mg $m^{-3}$) (Bosc et al., 2004).

From all the preceding considerations, ~~we finally concluded that~~ mid-April to mid-June was the target period for the cruise.

## 4. Spatial consideration: transect of principle of the PEACETIME cruise.

The central Mediterranean Sea (MS) ~~was our main targeted area since~~ all the marine ecoregions of the MS can be found in a relatively small ~~zone~~ (figure 4). Each ecoregion ~~detected on that figure~~ presents ~~a~~ characteristic ~~species association~~ from primary producers to top predators ~~of the epipelagic domain~~, forced by similar environmental conditions (Reygondeau et al., 2014). ~~As seen in figure 4,~~ the initial transect designed for PEACETIME aimed at visiting most of the identified ecoregions within the 4 weeks of cruise, ~~allowing us to test the impact of atmospheric deposition on a large range of natural assemblages.~~ The planned long stations of the transect of

principal were located within or at the center of 3 main ecoregions. Short stations (occupation time was less than 6 hours) were ~~positioned in order that cruising between two stations was long enough~~ (~8 hours) to allow the continuous measurement of both lower atmosphere and surface seawater while cruising. ~~Depending on atmospheric conditions during the cruise, it was anticipated that one of the long station (named FAST) would be dedicated to documenting a strong deposition event at sea, and that the forecasted occurrence of such an event would prompt a fast action plan that might lead to change the planned transect and ship route~~.

~~It has to be noted that~~ the coastal climate observatory of the Italian National Agency for New Technology, Energy and Environment (ENEA) on Lampedusa Island (35°31'06"N, 12°37'48"E; figure 5) could provide an excellent support ~~for~~ atmospheric conditions in the central basin before and during the cruise. ~~Indeed,~~ continuous measurements of aerosols concentrations (Marconi et al., 2014) and composition (Becagli et al., 2012 and 2013), nutrients deposition (Galletti et al., this issue), dust deposition (Vincent et al., 2016), optical measurements (Meloni et al., 2007) and the vertical distribution of aerosols in the atmospheric column by lidar (e.g. Di Iorio et al., 2009) ~~are conducted~~ at this site. During the cruise, 15 AERONET stations (Holben et al., 1998) ~~plotted~~ in figure 5 also provided continuous daytime measurements of the spectral aerosol optical depth (AOD).

## 5. Implementation of the PEACETIME cruise

Based on the scientific ~~arguments~~ detailed above and ~~on the availability of~~ the ship, the PEACETIME cruise was ~~conducted~~ during late spring ~~conditions from~~ May 10 to June 11, 2017 on board the R/V *Pourquoi Pas ?* Along ~~the~~ 4300 km transect, 10 short stations (with an average duration of 8 hours) and 3 long stations (respectively 4 days, 4 days and 5 days duration) ~~were occupied (~~figure 5 and table 1).

Everyday, thanks to the PEACETIME Operation Center (POC; see next section) ~~based on land~~, the ~~relevance to follow the~~ initial track was ~~discussed in the view of several types of~~ available or derived products from various operational centers producing model forecasts and near-real time remote sensing products~~). Figure 5 represents~~ both ~~the~~ planned and realized transect ~~following~~ the day-to-day adaptive strategy.

### 5.1 **Tools for decision: the PEACETIME Operation Center**

Based on the experience of the ChArMEx airborne campaigns (Mallet et al., 20016) and of previous oceanographic cruises needing an adaptive planning strategy based on observations and short-term forecasts (see section "Satellite monitoring of the ocean"), an operational server named the PEACETIME Operation Center (POC; http://poc.sedoo.fr/; last access 9 Feb. 2020) was set-up by the Service de Données de l'Observatoire Midi-Pyrénées (OMP/SEDOO, Toulouse, France) ~~for the cruise~~. It operated from early May to mid-June 2017, gathering a set of quick-looks of (i) near-real time selected remote sensing or other observational products and (ii) meteorological and chemistry-transport model forecasts, considered useful for the campaign planning decisions. The quick-looks were either directly transferred to the POC following their production by respective operational centers, or linked from their original browser. Various reports were also produced and made available on a quasi-daily basis ~~(~~meteorology and dust over the basin, regional and local oceanographic conditions (SPASSO; see hereafter), ~~ship trajectory..~~. The complete series of reports is available at http://poc.sedoo.fr/source/indexGarde.php?current=20170602&nav=Reports (last access 9 Feb. 2020). In the following, more details will be given on products that were found the most useful for daily decisions during the cruise.

The actual position~~s~~ of stations ~~were discussed~~ and determined on the basis of near-real time satellite data analysis (SPASSO, see later) in order to account for local oceanic conditions (~~i.e.~~

presence ~~or not~~ of mesoscale structures). In ~~parallel~~, short- and middle-term forecast models of weather conditions and of dust transport and deposition were systematically analyzed to verify the conditions, and eventually start the Fast Action. ~~The Fast Action strategy consisted in routing the ship towards an area of forecasted dust deposition event in order to tentatively document the respective roles of dynamics and deposition on marine biogeochemical conditions.~~ The goal was to position the ship in the center of ~~the~~ area of dust deposition, at least one day (24 hours) before the event in order to sample the water column before, during and after the ~~deposition, and collect and characterize the rain event.~~ Several constraints had to be considered for the Fast Action decision:

1. the uncertainties of the operational forecast models, which increased proportionally to the length of the forecasted period;
2. the ~~relative~~ position of the ship ~~(which was following the initial plan) and~~ the forecasted area of deposition, ~~accounting for the maximum cruise speed of the ship (i.e. 15 knots)~~ and the need to be positioned at the station 24 h before the deposition event;
3. national and international authorisations related to the EEZ (Exclusive Economic Zones)~~;~~, the Mediterranean ~~area~~ is almost completely submitted to national EEZ of surrounding countries ~~and~~, consequently, international oceanic areas are very scarce~~;~~, ~~a~~authorisation to sample an EEZ ~~should be demanded in advance to the corresponding country (generally~~ 24 h or 48 h before, depending on the country).

~~All these elements were simultaneously analysed during a daily meeting between scientists involved on land and on ship, as well as with the crew. Each day, the initial plan was confirmed for the next 48 h or, eventually, modified.~~ For most of the cruise (~~see~~ figure 5), only slight modifications of the initial plan were ~~decided~~, as atmospheric conditions were not considered favorable for the Fast Action. They dramatically changed on the 28th of May, during the

sampling of the ION station, ~~conducting to the decision to start~~ the Fast Action. ~~The sequence of events leading to the Fast Action are~~ described later.

**Atmospheric conditions**

Several near-real time remote sensing products and model forecasts ~~were used. In terms of aerosol remote sensing, we mainly relied on~~ two ~~products~~. The first one was the aerosol optical depth at 550 nm ($AOD_{550}$) ~~distribution over the sea~~, as produced in near-real time by the ICARE data and service centre, Lille, France (product SEV_AER-OC-L2; http://www.icare.univ-lille1.fr/projects/seviri-aerosols; last access 9 Feb., 2020). Data from the Spinning Enhanced Visible and Infra-red Imager (SEVIRI) on-board the geostationary satellite Meteosat Second Generation (MSG) are directly acquired every 15 min by the Service d'Archivage et de Traitement Météorologique des Observations Satellitaires of the Centre de Météorologie Spatiale (CMS/SATMOS), Lannion, France, and processed within hours by ICARE based on the algorithm of Thieuleux et al. (2005). The MSG satellite position at 0° longitude allows a good coverage for aerosol climatologies and case studies of aerosol transport over the Mediterranean basin (e.g. figure I.19 in Lionello et al., 2012; Chazette et al., 2016 and 2019) and surrounding continental regions (Carrer et al., 2014) as well as of desert dust source regions in Africa (e.g. Gonzales and Briottet, 2017). In addition to the quick-look from the level-2 product (SEV_AER-OC-L2) available between 4:30 and 18:00 UT ~~at the maximum~~ in mid-June in our area of interest, a daily mean level-3 (SEV_AER-OC-D3) is produced every night by averaging all available time slots during the previous day between 4:00 and 19:45 UT. ~~Figure 6 illustrates this product for the 3rd of June when an African dust plume from North Africa associated to a cloudy air mass invaded the westernmost Mediterranean basin atmosphere.~~ The horizontal resolution of the product is of 3 x 3 $km^2$ at nadir, of the order of 12.5 $km^2$ in the Alboran Sea, 15 $km^2$ in the North of the Gulf of Genova, and 18 $km^2$ in the northeasternmost

basin (about 13.07, 13.64, and 13.96 at the FAST, ION, and TYR station, respectively). Although less accurate than AOD from MODIS when compared to AERONET data, the high temporal resolution of MSG/SEVIRI-derived AOD offers a much better daily coverage of the area than any orbiting satellite (Bréon et al., 2011), especially when partial cloud coverage can be compensated thanks to successive images, ~~as illustrated in~~ figure 6.

The second ~~useful~~ remote sensing product was the North African Sand Storm Survey (NASCube) also produced ~~from~~ MSG/SEVIRI, at the Laboratoire d'Optique Atmosphérique, Lille, France (http://nascube.univ-lille1.fr; last access, 9 Feb. 2020). It generates continuous day and night images of desert dust plumes over the northern African continent and Arabian Peninsula, using an artificial neural network methodology producing colour composite images by processing 8 visible, near-infrared and thermal infrared bands of SEVIRI (Gonzales and Briottet, 2017). ~~Figure 7 shows~~ a window of this product for the 1st June 2017, show~~ing~~ the probable dust source regions (south of Morocco and western Algeria) of the plume found the following days over the westernmost Mediterranean basin ~~as~~ seen in figure 6.

During the campaign, we also used on a regular basis air mass trajectories computed with the Hysplit tool of the Air Resources Laboratory of the National Ocean and Atmosphere Administration (NOAA/ARL; https://ready.arl.noaa.gov/HYSPLIT_traj.php; last access 9 Feb. 2020; Stein et al., 2015; Rolph et al., 2017) based on global meteorological 192-h forecasts from the Global Forecasting System (GFS) model (1-deg, 3-h resolution) operated by the National Centers for Environmental Prediction (NCEP; Yang et al., 2006). It ~~could be~~ used both in forward mode to forecast the transport over the western Mediterranean of dust plumes detected over Africa by NASCube, and in backward mode to identify the origin of air masses over the ship position.

In addition to aerosol remote sensing observations we also used near real time rainfall remote sensing ~~produced~~ ~~by~~ the Meteo Company, an international weather network (https://meteoradar.co.uk; last access 9 Feb. 2020) providing ~~every 15 mn~~ real time weather radar- and satellite-derived maps of precipitation, clouds, and lightning on a European window covering most of the Mediterranean basin (north of 32°N or 35.5°N, depending on product~~s~~). ~~The~~ satellite infrared images from SEVIRI ~~are~~ filtered to show the thicker clouds, and observations from 45 European rain radar ~~are integrated~~. Figure 8 illustrates the combined SEVIRI satellite and radar product showing both clouds, precipitation and lightning for two time slots on 3 June 2017. They show the beginning and the end, respectively, of a convective rainfall of low intensity (<2 mm h-1) between Algeria and Spain in the dusty and cloudy area visible in Figure 6 west of the ship.

A number of operational forecast models were also used, both for weather forecast and aerosol transport. In order to understand the synoptic circulation, we especially considered surface pressure (*P*) and 500-hPa (about 5.5-km altitude) geopotential (*Z500*) maps over the European domain covering the whole Mediterranean basin and northern Atlantic from the global numerical weather prediction model ARPEGE (Courtier and Geleyn, 1988), developed and maintained at Météo-France. Its horizontal resolution varies from 7.5 km in France to 37 km over Southern Pacific, and four daily forecasts including data assimilation are carried out every day (available by http://www.meteociel.fr, last access 9 Feb. 2020). ~~Because we were especially targeting possible~~ aerosol deposition events, ~~we also analysed daily a set of up to 5-days, 1-, 3-, or 6-hourly depending on models,~~ precipitation forecasts from several models ~~including those~~ made available by meteociel.fr ~~including~~ global ~~weather forecast~~ models such as ARPEGE, IFS (the model developed at ECMWF; Barros et al. 1995), the Canadian CMC-MRB GEM model (Côté and Gravel, 1998), the GFS atmospheric model from NCEP

(Kanamitsu, 1989) and its ensemble GEFS, but also the regional non-hydrostatic model AROME (Seity et al., 2011) for the NW Mediterranean ~~only~~ at 1.3 km resolution.

Three regional dust transport models have also been considered, namely SKIRON operated by the Atmospheric Modeling and Weather Forecasting Group (AM&WFG) of the University of Athens (Kallos et al., 2009; Spyrou et al., 2010) and the two models NMMB-BSC (Non-Hydrostatic Multiscale Model; Pérez et al., 2011) and BSC-DREAM8b (Basart et et al., 2012) operated by the Barcelona Supercomputing Centre (BSC). SKIRON and BSC-DREAM8b have a horizontal resolution of 0.24° and 0.33°, respectively, and are both initialized and constrained at their boundaries by NCEP/GFS 6-hourly data. NMMB-BSC regional model has a resolution of 0.47° x 1/3° and is constrained by the NCEP global version of the model (Pérez et al., 2011).

~~In terms of dust transport modeling, we mainly relied on 6-hourly~~ dust optical depth and dry and wet dust deposition fluxes forecasted daily from 12 UTC ~~over~~ the ~~next~~ 72 h by the NMMB-BSC-Dust and BSC-DREAM8b v2.0 models and ~~over~~ the ~~next~~ 180 h (5.5 d) by SKIRON. ~~Because of its longer temporal range of forecast,~~ the wet dust deposition product by SKIRON was particularly useful to issue an early pre-alert for the Fast Action during the cruise. Figure 9 ~~compares~~ the forecast maps of ~~6-h~~ accumulated dust deposition flux ~~at 4 time steps~~ from ~~3rd~~ June 2017 12 UTC to ~~5~~ June 00 UTC, from the ~~2nd June~~ runs of those 3 models. ~~This period corresponds~~ to the scavenging of the dust plume shown in Figure 6 that was targeted for the Fast Action (~~see~~ below).

We also used a set of forecast of aerosol or dust optical depth from a series of models~~: (i) 60-h, 6-hourly ensemble and comparative forecasts of dust optical depth from models~~ operated by the BSC for the World Meteorological Organization (WMO) Sand and Dust Storm Warning Advisory and Assessment System (SDS-WAS), and made available by the Spanish Agencia Estatal de Meteorologia (AEMET; https://sds-was.aemet.es/forecast-products/dust-forecasts/;

last access 9 Feb. 2020; it is worth noting that Basart et al. (2016) model data comparison over summer 2012 showed better average performances of the model ensemble dust forecasts compared to forecasts from any individual model (ii) 5-days, 3-hourly dust and sulphate AOD Copernicus/GMES products over Europe and North Africa produced by the European Center for Medium-Range Forecast (ECMWF), and (iii) 114-h, 6-hourly sulfate, dust and smoke AOD over Europe and the Mediterranean region north of 35°N from the Naval Research Laboratory (NRL) global NRL Aerosol Analysis and Prediction System (NAAPS) model that is using an AOD assimilation package (Zhang et al., 2008); ~~further~~, we used the kml formatted animations of the NAAPS 5-days global forecasts of AOD projected on a GoogleEarth satellite view centered on the western Mediterranean, ~~which shows areas with significant AOD (>0.1) of sulfate, dust or smoke~~. Finally, we also considered the daily maps (at time 00 UTC) produced by the Earth Wind Map community (https://earth.nullschool.net; last access 9 Feb. 2020), consisting of AOD from sulfate or dust from the NASA Global Modeling and Assimilation Office (GMAO) Goddard Earth Observing System version 5 (GEOS-5) model overlaid by surface or 700 hPa winds from the GFS model in order to check the dominant aerosol type and transport conditions at the ship position.

**Ocean conditions**

~~Concerning the surface ocean,~~ several remote-sensing datasets ~~were exploited using the~~ SPASSO (Software Package for an Adaptive Satellite-based Sampling for Ocean campaigns https://spasso.mio.osupytheas.fr/; last access: 9 Feb. 2020) in order to guide the cruise through a Lagrangian adaptive sampling-strategy aiming at avoiding region of complex circulation and dynamics (fronts, small scale eddies). ~~The idea behind~~ this approach ~~was to aim at~~ a situation where the air-sea exchanges dominate and lateral advection and diffusion can be neglected. Such an approach was already successfully adopted during several previous cruises such as

LATEX (Nencioli et al., 2011; Doglioli et al., 2013, Petrenko et al., 2017), KEOPS2 (d'Ovidio et al., 2015), OUTPACE (Moutin et al., 2017; de Verneil et al., 2018) and OSCAHR (Rousselet et al., 2019). During PEACETIME, we used the following datasets: (~~1~~) altimetry data from the AVISO Mediterranean regional product (https://www.aviso.altimetry.fr/data/products/sea-surface-height-products/regional/mediterranean-sea-gridded-sea-level-heights-and-derived-variables.html); the altimetry-derived currents were then processed by SPASSO to derive Eulerian and Lagrangian diagnostics of ocean circulation: Okubo-Weiss parameter, particle retention time and advection, Finite Size Lyapunov Exposant (~~e.g.~~ figure 10); ~~(2) the~~ sea surface temperature (level 3 with resolutions of 4 and 1 km) and ~~(3)~~ the chlorophyll concentration (level 3 with a resolution of 1 km, MODIS Aqua and NPPVIIRS sensors combined after May 27, 2017 into a unique product) provided by CMEMS - Copernicus Marine Environment Monitoring Service (http://marine.copernicus.eu/).

### 5.2 The Fast Action

## The decision process and atmospheric conditions

On the 28th of May, the ship was ending the long station ION in the Ionian Sea under ~~a continuing northern~~ atmospheric flux. A low pressure system reaching Spain from the Atlantic, a typical situation for African dust transport in summer in this area (Moulin et al., 1998) caused a ~~southern flux~~ over the western basin. ~~But~~ no significant emission ~~of dust was yet~~ detected in Africa with NASCube. Aerosol transport models forecasted, however, the presence of dust plume of moderate intensity for the following days, mainly confined to the southern part of the western Mediterranean basin following a persistent ~~western~~ flux for several days limiting the extens~~ion~~ of dust transport towards the north of the basin. Some dust was predicted by NMMB-BSC and SKIRON model runs ~~of 27~~ June to be deposited by rain south of the Balearic islands on 30 and 31 May, but meteorological forecasts did not converge on the time and location of

precipitation. In addition, the possible area of dust deposition was far from the ship~~,~~ 16° ~~in longitude~~ west from the ION station. Consequently, no modification of the initial plan was decided and ~~the~~ station 8 ~~was carried out~~ southwest of Sicily on 30 May.

At the end of station ~~8 on 30th May,~~ satellite observations confirmed the presence of atmospheric dust in a cloudy air mass over the western part of the Mediterranean and long-term predictions of AOD indicated the continuing presence of dust over the Alboran Sea, with a new dust plume likely extending northwest on June ~~2 or 3~~. Although models still diverged ~~in forecasting rain~~ over this region, the southwestern part of the Mediterranean basin ~~looked to be~~ the most dusty ~~area~~ for the next days ~~and it was decided to modify~~ the initial plan ~~and to move towards~~ the west for the last part of the cruise (~~see figure 5, the~~ long transect south of Sicily).

~~The 31th of May the ship reached a position approximately located between Sicily and Sardinia islands.~~ Significant dust emissions were again observed over North Africa ~~from the night of~~ 30-31 May on, ~~and the~~ predictions for a new significant dust event over the southwestern Mediterranean ~~on~~ June ~~3-5 were confirmed.~~ Although the differences between the models were still ~~important~~ (only SKIRON forecasted a wet deposition event south of Spain for ~~the 3-4th~~ of June), it was decided to continuously move the ship westward~~,~~ and t~~o~~ shift station 9 from its initial position in the Tyrrhenian Sea to a new position in the Alboran Sea. ~~We considered that~~ another station in the Tyrrhenian area was not critical for the cruise objectives and ~~that~~ establishing the area of next operations in the Alboran Sea ~~could~~ facilitate ~~the~~ re-positioning ~~of the ship in the case of~~ a confirmed prediction of a wet deposition event.

~~The 1st of June,~~ during ~~the~~ sampling at station 9 midway between Sicily and Spain, ~~it was decided to start~~ the Fast Action. ~~Indeed,~~ dust emissions continued in Algeria and southern Morocco associated to a southern flux~~,~~ aerosol transport models confirmed a new significant dust episode with AOD >0.8 (i.e. roughly 1 g $m^{-2}$ of dust in the atmospheric column) ~~for~~ June

3-5, and the occurrence of associated rains appeared most likely from ~~most~~ meteorological forecasts. SKIRON and NMMB-BSC predicted ~~the dust~~ wet deposition ~~flux~~ to be more important on ~~3rd~~ June in the Alboran Sea west of 0° longitude~~,~~ of the order of 1.5 and 0.5 g $m^{-2}$, respectively)~~, but~~ longer-term forecasts by SKIRON predicted wet dust deposition ~~more~~ east south of the Balearic Islands ~~on June 4 (~0.5 g $m^{-2}$) and especially on first half of June 5 (possibly >1.5 g $m^{-2}$),~~ ~~a~~ possibility confirmed by other rain forecasts. The Fast Action station was positioned 145 km south the ~~Balearic~~ Island of Mallorca and 126 km north of the Algerian coast (Figure 5), where a limited portion of the ~~sea~~ is ~~part of~~ international waters (i.e. not ~~included~~ in an EEZ), and ~~in an area where~~ the influence of Atlantic waters ~~reacher in nutrients than Mediterranean waters~~ should be limited compared to the more western Alboran Sea. The ship reached the FAST station location on the 2nd of June at the end of the day (Table 1) and the ocean and atmospheric sampling started immediately.

Although cloudy~~,~~ only from the 3rd of June ~~rain conditions were~~ observed in the neighbouring area (~~see rain radar composite images in~~ figure 11). ~~The~~ SEVIRI AOD ~~remote sensing~~ confirmed the export of a dust plume from North Africa south of the Balearic Islands ~~with high AOD~~ (>0.8; Figure 6) and NASCube confirmed new dust emissions in the night from 3 to 4 June. The dust plume was transported to the NE ~~up to~~ Sardinia on June 4~~,~~ with AOD <0.5 in all the area ~~and clear sky with low AOD~~ ~~was left~~ west of 4°E on June 5 (Desboeufs et al., in preparation, this issue). Wet deposition of dust for the 4th and early 5th June in the FAST station area were confirmed by ~~the deposition maps from the~~ 3 regional dust transport model forecast runs of June 2, although with decreasing intensity compared to the previous runs (except for BSC-DREAM8b that did not forecast dust wet deposition in earlier run)~~,~~ from a very small flux ~~of~~ a few mg $m^{-2}$ (BSC-DREAM8b) to about 100 mg $m^{-2}$ (NMMB-BSC) and up to more than 1 g $m^{-2}$ (SKIRON) (Figure 9). A rain front, moving eastward from Spain and North Africa

regions, reached the Fast Action position the night between ~~the~~ 4th and ~~the~~ 5th of June (Figure 11). A single ~~event of~~ rain was observed and sampled ~~on the ship~~ at the station FAST on ~~5th~~ June from 2:36 am to 3:04 am. Continuous lidar measurements on board the ship confirmed the presence of a dust layer ~~mainly~~ over the atmospheric boundary layer ~~over~~ the FAST station and ~~its~~ below-cloud deposition during the rain event ~~of~~ early ~~5th~~ June (Desboeufs et al., in preparation, this issue). The chemical composition of this rain sample confirmed wet deposition of dust reaching a total particulate flux of 12 $mg.m^{-2}$ (Fu et al., in preparation, this issue), which is among the lowest most intense dust deposition fluxes recorded in this area from long time-series of deposition network (Vincent et al., 2016).

## Sea Surface dynamic context at FAST

Several approaches have been implemented to highlight ~~the~~ dynamical context around the FAST station ~~in the waters above 200m, the physical structures and~~ the possible influences of ~~the~~ dynamics on the stability of the water masses at the station. These approaches are based on in situ observations (Moving Vessel Profiler (VMP) transect and drifters trajectories) and diagnostic tools.

On board, a MVP collected high frequency Conductivity- Temperature- Depth (CTD) data along two transects: the first one when the vessel approached the FAST station from the east, before the station took place, and the second one west of the FAST station, on the transect back from station 10~~.~~ Figure 12 ~~shows these data in a longitude-depth section.~~ To the east of the FAST station the surface water was colder and saltier than to the west, where ~~a strong deformation of~~ the isopycnals ~~suggests~~ the presence of an Algerian anticyclonic eddy. Such eddy carries ~~recent~~ Atlantic water and generates a southward current that only partially ~~impacts~~ the FAST station area.

The post-cruise comparison of the hull-mounted ADCP data combined with the SVP drifters trajectories and the altimery-derived currents shows a good agreement ~~all along the~~ cruise and in particular at the FAST station (Figure 12). Moreover, the agreement between SVP and numerical particle trajectories ~~has been~~ slightly improved when ~~we also took into account the~~ Ekman drift ~~calculated~~ with wind data from the high resolution regional model WRF 3.7.

This allowed us to ~~calculate~~ backward trajectories of ~~the~~ surface water masses using the ARIANE Lagrangian tool (Blanke and Raynaud, 1997; Blanke et al., 1999) in order to estimate the origins of the sampled ~~surface water~~ at the LD stations. ~~As seen from the repeated CTDs (see previous section), at the FAST station a southward current associated to the large Algerian eddy was present~~. We estimated that ~~over the whole station duration, a mean value of 57(26)%~~ of water ~~remained in the station zone~~ after 1~~(2)~~ day~~(s). Moreover,~~ combining the particle trajectories and the precipitation data from the WRF 3.7 model we concluded that the rain, which fell slightly upstream ~~the LD-FAST~~ station in the previous days, likely impacted the sampled water mass (figure 14).

## Temporal evolution of surface seawater properties during FAST

~~Station FAST has been documented at its fixed point during seven days by 43 repeated CTD casts in the depth range 0-200 m.~~

~~The hydrological situation was~~ characterized by a very shallow surface mixed layer and a sharp seasonal thermocline that extended ~~underneath~~ down to 75 m depth (Figure 15, upper ~~right~~ and middle right panels). In th~~is~~ upper layer, salinity values were lower than 37.5, ~~which is~~ characteristic of modified Atlantic waters flowing eastward inside the Mediterranean Sea. In ~~the~~ deeper layers, salinity increased sharply ~~with depth until~~ 350 m where it reached ~~its~~ maximum value ~~(~~38.59~~)~~, ~~which is characteristic~~ of Levantine intermediate waters flowing

westward into the Mediterranean outflow. Deep waters, formed ~~at~~ winter convection zones of the northwestern Mediterranean, had lower salinity values (38.48)~~; they extended~~ from 1400 m down to the sea bottom.

The hydrological conditions at this site ~~between June~~ 2 ~~and~~ 8 ~~during the Fast Action mainly~~ evolved in the upper layer (Figure 15, upper ~~left~~ and middle left panels). The surface mixed layer ~~was shallow with variations from~~ 9-m to 19-m ~~depth~~ following the diurnal cycle. Mixed layer salinity remained ~~equal~~ until the 7$^{th}$ of June~~; in particular~~ no dilution effect ~~due~~ the rainfall on 3$^{rd}$ June ~~has been recorded. The~~ stratification of the whole water column remained ~~steady~~ during the long station. Density horizons ~~kept lain~~ along isobars in the upper layer, ~~which signs the~~ absence of geostrophic perturbations during the long station. However, ~~the~~ current profilers indicated a depth-independent (barotropic) motion of amplitude 3 cm s$^{-1}$ heading 220°, which is in agreement with the position of the station within the large eastern Algerian ~~Gyre, a component of the basin scale cyclonic circulation described by~~ Testor et al. ~~(~~2005). This southwestward flow ~~transported~~ ~~superficial~~ water masses of distinct properties ~~as clearly marked below the mixed layer by~~ salinity anomalies (~~referenced to the initial profile of 2$^{nd}$~~ June 16:30). These water masses crossed the observation site, disrupting the water column in the depth range of 25-100 m, lowering salinity values by 0.1 in the extension of the thermocline and increasing salinity values by 0.05 underneath. Al~~though clearly present,~~ this ~~hydrological~~ anomaly did not affect the surface waters ~~and~~ the ~~MLD was stable~~ during ~~the Fast Action~~ preclud~~ing~~ any input from below that could have been linked to destratification induced by strong wind associated to the dust event ~~as hypothesized in Guieu et al. (2010) from time-series observations in the northwestern Mediterranean Sea.~~ Such conditions ~~are~~ favorable to observe any change strictly attributed to external inputs from above ~~(i.e. atmospheric deposition)~~.

~~The distribution of phytoplanktonic biomass has been detected by optical sensors mounted in the CTD package (Figure 15 lower panels):~~ measurements of fluorescence and ~~of~~ beam ~~transmission provided~~ similar patterns, stressing the biogenic character of particles present in the water column. Intermittent signal at the sea surface ~~has been~~ detected only by transmissometry, ~~however~~ no clear relationship with the rainfall event ~~can be stated~~ (see the first profile after event in red). ~~The vertical distribution was~~ displayed ~~as~~ a deep chlorophyll maximum of about 20-m thickness~~,~~ located at the base of the thermocline (about 75 m). ~~Short-term evolution~~ during the seven days of observation displayed variations in intensity and depth ~~of the deep chlorophyll maximum, as well as splitting and merging sequences of the peak.~~ Such perturbations appeared after the rainfall event ~~of the~~ ~~3rd~~ June, however they more likely result from the intrusion of water masses from north at this depth range. This hypothesis is reinforced by the absence of any geostrophic perturbation in the density time series that could have injected biomass or nutrients via diapycnal processes. Another candidate could be the mixing effect associated to the breaking of internal gravity waves that propagated along the thermocline.

~~5.3 Work at stations and work underway~~

~~In the figure 16 we show the satellite-derived SST data averaged taking into account the ship position.~~ During the cruise a general warming of the sea surface ~~is~~ observed and the FAST station has been performed in waters warmer than the two others LD stations.

Chlorophyll concentrations as seen by satellite over the western and central Mediterranean Sea were typical of the oligotrophic conditions encountered during the season characterized by ~~a~~ strong stratification (Figure 17). ~~The~~ west-east gradient ~~between~~ oligotrophic to very oligotrophic ~~was clearly established and minimal~~ concentrations ~~(about 0.05 mg m$^{-3}$ ) were observed~~ in the Ionian Sea.

~~Surface inorganic nutrients measured at nanomolar concentrations were very low for both dissolved inorganic nitrogen (DIN) and phosphorus (DIP). Indeed,~~ average concentration in ~~0-~~ 20 m ~~layer was~~ 90 nM DIN and 15 nM DIP at the westernmost station (station 10) and 14 nM DIN and 10 nM DIP at the easternmost station (ION). Along the longitudinal transect, a deepening of the nutrient depleted layer toward the east was observed (figure 18) consistent with the general trend of those nutrients in the Mediterranean basin as described in Mermex Group (2011) ~~and references inside.~~

~~All along the cruise, the work at sea was divided between short (~8 hours) and long (up to five days) stations to allow both a good description of the different ecoregions crossed and to perform process studies. The number of short stations was the best compromise in order to (1) allow at least 8 hours of transect at 9 knots in between 2 short stations, necessary for a good continuous monitoring of both low atmosphere and surface waters while cruising and (2) to have enough short stations to describe well enough stocks and fluxes along the whole column water and microstructure of the mixed layer in the contrasted biogeochemical regions crossed. Long stations were located in 3 different ecoregions (see Figure 3) characterized by different *in situ* conditions (see figures 16 & 17) all characterized by oligotrophic conditions. The duration of the long stations (4 days at TYR and ION and 5 days at FAST; table 1) allowed process studies both in situ (drifting mooring supporting different types of traps and instruments) and on board (artificial dust seeding experiment in 300 L climate reactors; see below). Table 2 summarizes the operations conducted during the cruise and the parameters obtained, (1) on a continuous basis, (2) at short stations, and (3) at long stations . A summary of the use of those parameters in the different papers presented in this Special Issue and in other papers is also given in that table.~~

## 6. Conclusion

The PEACETIME oceanographic expedition conducted in spring 2017 cruised over a ~~20°~~ longitudinal gradient across the western and central Mediterranean Sea during ~~the~~ season characterized by strong stratification, low productivity and high chance to be ~~submitted to~~ dust wet deposition. Those conditions were required in order to fulfil the objectives of the project aiming at quantifying the biogeochemical processes at play after atmospheric deposition and its impact on ecosystem functioning. Thanks to an adaptive strategy based on a large panel of atmosphere and ocean real time observations and forecast models, the ~~track of the~~ cruise ~~was~~ optimized from day to day. In particular, ~~we were successful to timely reroute~~ the R/V toward an area where dust deposition was expected and actually observed and sampled. Different atmospheric situations were encountered during the ~~cruise~~, allowing the acquisition of a large dataset under different dynamical and biogeochemical ~~in situ~~ conditions to explore the chemical and ecosystem in situ response to deposition.


## Acknowledgments

This study is a contribution to the PEACETIME project (http://peacetime-project.org), a joint initiative of the MERMEX and ChArMEx components supported by CNRS-INSU, IFREMER, CEA, and Météo-France as part of the programme MISTRALS coordinated by INSU. PEACETIME was endorsed as a process study by GEOTRACES. PEACETIME cruise https://doi.org/10.17600/17000300. We thank the captain and the crew of the RV *Pourquoi Pas ?* for their professionalism and their work at sea. We warmly thank Louise Rousselet, Alain de Verneil, and Alice Della Penna for their precious help with SPASSO and the daily bulletins, Hélène Ferré from OMP/SEDOO for her management of the Peacetime Operation Center, and Louis Prieur for fruitful discussion on the characterisation of the ocean processes observed at

the station FAST. We finally acknowledge the technical help of the many teams supporting operational production of model forecasts and remote sensing products that contributed to the POC and were the basis of our daily briefings and decision for the Fast Action, ~~especially~~ Jacques Descloitres for MSG-derived AOD, Louis Gonzalez for NASCube products, and Christos Spyrou for SKIRON forecasts.

**Author contribution:** CG and KD designed the PEACETIME project. FD and FDO analyzed the FAST Action. FD, MM and PN analysed the atmospheric components and VT, AD, AP and SB analysed the marine components. CG prepared the manuscript with contributions from all co-authors.

## References

1. Avila, A., Queralt-Mitjans, I., & Alarcón, M. (1997) Mineralogical composition of African dust delivered by red rains over northeastern Spain, J. Geophys. Res., 102, 21977-21996, doi:10.1029/97JD00485.
2. Barbieux M., Uitz J., Mignot A., Gentili B., Roesler C., Loisel H., Poteau A., Schmechtig C., Taillandier V., Leymarie E., Penkerc'h C., Claustre H., D'Ortenzio F. & Bricaud A., Subsurface biological production in the Mediterranean Sea: Estimates based on the diel cycle of optical properties measured by BGC-Argo floats, in preparation (this special issue)
3. Barros, S.R.M., Dent, D., Isaksen, L., Robinson, G., Mozdzynski, G., & Wollenweber, F. (1995) The IFS model: A parallel production weather code, Parallel Computing, 21, 1621-1638, doi:10.1016/0167-8191(96)80002-0.
4. Basart S., F. Dulac, J.M. Baldasano, P. Nabat, M. Mallet, F. Solmon, B. Laurent, J. Vincent, L. Menut, L. El Amraoui, B. Sic, J.-P. Chaboureau, J.-F. Léon, K. Schepanski, J.-B. Renard, F. Ravetta, J. Pelon, C. Di Biagio, P. Formenti, I. Chiapello, J.-L. Roujean, X. Ceamanos, D. Carrer, M. Sicard, H. Delbarre, G. Roberts, W. Junkermann, & J.-L. Attié (2016) Extensive comparison between a set of European dust regional models and observations in the western Mediterranean for the summer 2012 pre-ChArMEx/TRAQA campaign, In Air Pollution Modeling and its Application

XXIV, D.G. Steyn and N. Chaumerliac Eds., Springer Series Proc. in Complexity, 79-83, doi:10.1007/978-3-319-24478-5_13.

5. Basart S., Pérez, C., Nickovic, S., & Baldasano, J.M. (2012) Development and evaluation of the BSC-DREAM8b dust regional model over Northern Africa, the Mediterranean and the Middle East, Tellus, 64, 18539, doi:10.3402/tellusb.v64i0.18539.

6. Becagli, S., Lazzara, L., Fani, F., Marchese, C., Traversi, R., Severi, M., di Sarra, A., Sferlazzo, D. M., Piacentino, S., 461 Bommarito, C., Dayan, U., and Udisti, R. (2013) Relationship between methanesulfonate (MS−) in atmospheric 462 particulate and remotely sensed phytoplankton activity in oligo-mesotrophic central Mediterranean Sea, 463 Atmospheric Environment, 79, 681-688, https://doi.org/10.1016/j.atmosenv.2013.07.032

7. Becagli, S., Sferlazzo, D. M., Pace, G., di Sarra, A., Bommarito, C., Calzolai, G., Ghedini, C., Lucarelli, F., Meloni, D., Monteleone, F., Severi, M., Traversi, R., and Udisti, R. (2012): Evidence for heavy fuel oil combustion aerosols from chemical analyses at the island of Lampedusa: a possible large role of ships emissions in the Mediterranean, Atmos. Chem. Phys., 12, 3479-3492, 10.5194/acp-12-3479-2012.

8. Bergametti G., E. Remoudaki, R. Losno, E. Steiner, B. Chatenet, & P. Buat-Ménard (1992) Source, transport and deposition of atmospheric phosphorus over the northwestern Mediterranean, Journal of Atmospheric Chemistry, 14, 501-513, doi:10.1007/BF00115254.

9. Bergametti, G., Dutot, A. L., Buat-Ménard, P., Losno, R., & Remoudaki, E. (1989) Seasonal variability of the elemental composition of atmospheric aerosol particles over the Northwestern Mediterranean, Tellus, 41B, 353-361, doi:10.1111/j.1600-0889.1989.tb00314.x.

10. Berline L, Doglioli AM, Petrenko A, Barrillon S, Simon-Bot F & Carlotti F, Sharp gradient in particle load at the boundary between Modified Atlantic Water and Ionian Surface Water, Central Ionian Sea, in preparation (this special issue)

11. Blanke, B., & Raynaud, S. (1997) Kinematics of the Pacific equatorial undercurrent: An Eulerian and Lagrangian approach from GCM results, Journal of Physical Oceanography, 27, 1038-1053, doi:10.1175/1520-0485(1997)027<1038:KOTPEU>2.0.CO;2.

12. Blanke, B., Arhan, M., Madec, G., & Roche, S. (1999) Warm water paths in the equatorial Atlantic as diagnosed with a general circulation model, Journal of Physical Oceanography, 29, 2753-2768, doi:10.1175/1520-0485(1999)029<2753:WWPITE>2.0.CO;2.

13. Bonnet, S., & Guieu, C. (2006) Atmospheric Forcing on the Annual Iron Cycle in the Mediterranean Sea. A one-year Survey. Journal of Geophysical Research, 111, C09010, doi:10.1029/2005JC003213.

14. Bosc, E., Bricaud, A., & Antoine, D. (2004) Seasonal and interannual variability in algal biomass and primary production in the Mediterranean Sea, as derived from 4 years of SeaWiFS observations, Global Biogeochemical Cycles, 18, GB1005, doi:10.1029/2003GB002034.

15. Brandt M.I, Trouche B., Quintric L., Wincker P., Poulain J., Arnaud-Haond S., A flexible pipeline combining bioinformatic correction tools for prokaryotic and eukaryotic metabarcoding. https://doi.org/10.1101/717355, submitted, 2019

16. Brandt M.I., Zeppilli D., Simier M., Guenther B., Trouche B., Henry N., Orejas C., Pradillon F., Fabri M-C, Cambon-Bonavita A-M, Guieu C., Quintric L., Belser C., Poulain J., Wincker P., Maignien L., de Vargas C., & Arnaud-Haond S., Multi-marker eDNA metabarcoding reveals large and small-scale metazoan biodiversity patterns in the deep-sea Atlantic-Mediterranean transition zone, in preparation.

17. Bréon, F.-M., Vermeulen, A., & Descloitres, J. (2011) An evaluation of satellite aerosol products against sunphotometer measurements, Remote Sensing of Environment, 115, 3102-3111, doi:10.1016/j.rse.2011.06.017.

18. Bressac M, Wagener T, Tovar-Sanchez A, Ridame C, Albani S, Fu F, Desboeufs K & Guieu C, Residence time of dissolved and particulate trace elements in the surface Mediterranean Sea (Peacetime cruise), in preparation (this special issue)

19. Bressac M., C. Guieu, D. Doxaran, F. Bourrin, N. Leblond K. Desboeufs & C. Ridame (2014) Quantification of the lithogenic carbon pump following a simulated dust deposition event in large mesocosm, Biogeosciences, 11, 1007-1020, doi:10.5194/bg-11-1007-2014.

20. Bressac M., C. Guieu, M. J. Ellwood, A. Tagliabue, T. Wagener, E. C. Laurenceau Cornec, H. Whitby, G. Sarthou, & P. W. Boyd. (2019) Resupply of mesopelagic dissolved iron controlled by particulate iron composition. Nature Geoscience, 12(12), 995:1000, doi:10.1038/s41561-019-0476-6.

21. Bressac, M., & Guieu, C. (2013) Post-depositional processes: What really happens to new atmospheric iron in the ocean surface? Global Biogeochemical Cycles, 27, 859-870, doi:10.1002/gbc.20076.

22. Carrer D., X. Ceamanos, B. Six, & J.-L. Roujean (2014) AERUS-GEO: A newly available satellite-derived aerosol optical depth product over Europe and Africa, Geophysical Research Letters, 41, 7731-7738, doi:10.1002/2014GL061707.

23. Chazette, P., Totems, J., & Shang, X. (2019) Transport of aerosols over the French Riviera – link between ground-based lidar and spaceborne observations, Atmospheric Chemistry and Physics, 19, 3885–3904, doi:10.5194/acp-19-3885-2019.

24. Chazette, P., Totems, J., Ancellet, G., Pelon, J., & Sicard, M. (2016) Temporal consistency of lidar observations during aerosol transport events in the framework of the ChArMEx/ADRIMED campaign at Minorca in June 2013, Atmospheric Chemistry and Physics, 16, 2863–2875, doi:10.5194/acp-16-2863-2016.

25. Côté, J., S. Gravel, A. Méthot, A. Patoine, M. Roch, & A. Staniforth, 1998: The Operational CMC–MRB Global Environmental Multiscale (GEM) Model. Part I: Design Considerations and Formulation. Mon. Wea. Rev., 126, 1373–1395, doi:10.1175/1520-0493(1998)126<1373:TOCMGE>2.0.CO;2.

26. Courtier, P. & Geleyn, J.-F. (1988) A global numerical weather predic-tion model with variable resolution: Application to the shallowmodel equations, Q. J. Roy. Meteor. Soc., 114, 1321–1346, doi:10.1002/qj.49711448309.

27. de Verneil, A., Rousselet, L., Doglioli, A. M., Petrenko, A. A., Maes, C., Bouruet-Aubertot, P., & Moutin, T. (2018) OUTPACE long duration stations: physical variability, context of biogeochemical sampling, and evaluation of sampling strategy, Biogeosciences, 15, 2125–2147, doi:10.5194/bg-15-2125-2018.

28. Desboeufs K, J.-F. Doussin, C. Giorio, S. Triquet, F. Fu, D. Garcia-Nieto, F. Dulac, A. Féron, P. Formenti, F. Maisonneuve, V. Riffault, A. Saiz-Lopez, G. Siour, P. Zapf & C. Guieu, ProcEss studies at the Air-sEa Interface after dust deposition in the MEditerranean sea (PEAcEtIME) cruise: Atmospheric and FAST ACTION overview and illustrative observations, in preparation (a) (this special issue)

29. Desboeufs K., C. Giorio, S. Triquet, V. Riffault, P. Chazette, J. Dinasquet, F. Dulac, F. Fu, G. Siour, K. Sellegri, J. Dinasquet, D. García-Nieto, A. Doglioli, P. Formenti, A. Saiz-Lopez, C. Guieu and J.-F. Doussin, New particle formation in the marine

boundary layer after wet Saharan dust deposition in the Mediterranean Sea, in preparation (b)

30. Desboeufs K., N. Leblond, T. Wagener, E. Bon Nguyen & C. Guieu (2014) Chemical fate and settling of mineral dust in surface seawater after atmospheric deposition observed from dust seeding experiments in large mesocosms, Biogeosciences, 11, 5581-5594, doi:10.5194/bg-11-5581-2014.

31. Desboeufs, K., Bon Nguyen, E., Chevaillier, S., Triquet, S., & Dulac, F. (2018) Fluxes and sources of nutrient and trace metal atmospheric deposition in the northwestern Mediterranean, Atmospheric Chemistry and Physics, 18, 14477–14492, doi:10.5194/acp-18-14477-2018.

32. Desgranges M-M, Petrova1 M.V., Dufour A., Oursel B., Layoun P., Guieu C., Point D., Sarthou G., Jacquet S., Heimbürger-Boavida L-E, Methylmercury: a new tracer for the remineralization of organic matter? in preparation (this special issue)

33. Di Iorio, T., di Sarra, A., Sferlazzo, D.M., Cacciani, M., Meloni, D., Monteleone, F., Fuà, D., & Fiocco, G. (2009) Seasonal evolution of the tropospheric aerosol vertical profile in the central Mediterranean and role of desert dust, Journal of Geophysical Research: Atmospheres, 114, D02201, doi:10.1029/2008JD010593.

34. Dinasquet J., Bigeard E., Obernosterer I. & Baudoux A-C., Impact of dust enrichment on the microbial food web under present and future conditions of pH and temperature, in preparation (this special issue)

35. Doglioli, A. M., Nencioli, F., Petrenko, A. A., Rougier, G., Fuda, J. L., & Grima, N. (2013) A software package and hardware tools for in situ experiments in a Lagrangian reference frame. Journal of Atmospheric and Oceanic Technology, 30, 1940-1950, doi:10.1175/JTECH-D-12-00183.1.

36. d'Ortenzio, F., Iudicone, D., de Boyer Montegut, C., Testor, P., Antoine, D., Marullo, S., Santoleri, R., & Madec, G. (2005) Seasonal variability of the mixed layer depth in the Mediterranean Sea as derived from in situ profiles, Geophysical Research Letters, 32, L12605, doi:10.1029/2005GL022463.

37. d'Ovidio, F., Della Penna, A., Trull, T. W., Nencioli, F., Pujol, M.-I., Rio, M.-H., Park, Y.-H., Cotté, C., Zhou, M., & Blain, S. (2015) The biogeochemical structuring role of horizontal stirring: Lagrangian perspectives on iron delivery downstream of the Kerguelen Plateau, Biogeosciences, 12, 5567–5581, 2015, doi:10.5194/bg-12-5567-2015.

38. Dulac F., C. Moulin, H. Planquette, M. Schulz, & M. Tartar (2004) African dust deposition and ocean colour in the eastern Mediterranean. Rapp. Comm. Int. Mer Médit., Vol. 37, 190, Commission Internationale pour l'Exploration Scientifique de la Méditerranée, Monaco.

39. Engel, A., Zäncker, B., Michels, J., Liebetrau, V. Interactions between organic matter and aeolian mineral dust in the sea surface microlayer, in preparation

40. Escudero, M., Castillo, S., Querol, X., Avila, A., Alarcón, M.,Viana, M. M., Alastuey, A., Cuevas, E., & Rodríguez, S. (2005) Wet and dry African dust episodes over eastern Spain, J. Geophys. Res., 110, D18S08, doi:10.1029/2004JD004731.

41. Feliu G., Pagano M., & Carlotti C. Structure and functioning of epipelagic mesozooplankton in the Mediterranean sea during spring peacetime cruise 2017, in preparation (this special issue)

42. Formenti, P., D'Anna, B., Flamant, C., Mallet, M., Piketh, S. J., Schepanski, K., ... & Chaboureau, J. P. (2019) The Aerosols, Radiation and Clouds in southern Africa (AEROCLO-sA) field campaign in Namibia: overview, illustrative observations and way forward, Bulletin of the American Meteorological Society, 100, 1277-1298, doi:10.1175/BAMS-D-17-0278.1.

43. Freney E., K. sellegri, A. Nicosia, M. Bloss, E. Asmi, M. Rinaldi, D. Lefevre, M. Thyssen, G. Gregori, K. Desboeufs & C. Guieu, High time resolution measurements of organic content and biological origin of Mediterranean sea spray aerosol (this special issue)

44. Fu F., Desboeufs K., Tovar-Sánchez A., Bressac M., Triquet S., Doussin J-F, Giorio C., Dulac F. & Guieu C., Solubility and concentration of trace metals and nutrients in wet deposition and impact on their marine concentration during PEACETIME cruise in the Mediterranean Sea, in preparation (b) (this special issue)

45. Fu F., Desboeufs K., Triquet S., Doussin J-F, Giorio C., Dulac F. & Guieu C., Solubility and sources of trace metals and nutrients associated with aerosols collected during cruise PEACETIME in the Mediterranean Sea, in preparation (a) (this special issue)

46. Fu, Y., Desboeufs, K., Vincent, J., Bon Nguyen, E., Laurent, B., Losno, R., & Dulac, F. (2017) Estimating chemical composition of atmospheric deposition fluxes from mineral insoluble particles deposition collected in the western Mediterranean region,

Atmospheric Measurement Techniques, 10, 4389–4401, doi:10.5194/amt-10-4389-2017.

47. Galletti, Y., S. Becagli, A. di Sarra, M. Gonnelli, E. Pulido-Villena, D.M. Sferlazzo, R. Traversi, S. Vestri, C. Santinelli, Atmospheric deposition of organic matter at a remote site in the 1 Central Mediterranean Sea: implications for marine ecosystem (this special issue)

48. Gallisai, R., Peters, F., Volpe, G., Basart, S., & Baldasano, J. M. (2014) Saharan dust deposition may affect phytoplankton growth in the Mediterranean Sea at ecological time scales. PloS ONE, 9, e110762, doi:10.1371/journal.pone.0110762.

49. Garcia-Nieto D., N. Benavent, Carlos A. Cuevas & A. Saiz-Lopez, MAXDOAS measurements of trace gases and aerosols over the Mediterranean Sea during the PEACETIME cruise, in preparation (this special issue)

50. Garel, M., Bonin, P., Martini, S., Guasco, S., Roumagnac, M., Bhairy, N., ... & Tamburini, C. (2019). Pressure-Retaining Sampler and High-Pressure Systems to Study Deep-Sea Microbes Under in situ Conditions. Frontiers in microbiology, 10, 453.

51. Gazeau F., Alliouane, S., Stolpe, C., Irisson, J.-O., Marro S., Dolan J., Blasco T., Uitz J., Dimier C., Grisoni J.-M., De Liège G., Hélias-Nunige S., Djaoudi K., Pulido-Villena E., Dinasquet J., Obernosterer I., Ridame C., & Guieu C. Impact of dust enrichment on Mediterranean plankton communities under present and future conditions of pH and temperature : an overview, in preparation (a) (this special issue)

52. Gazeau F., Marañon E., Van Wambeke F., Alliouane S., Stolpe C., Blasco T., Ridame C., Pérez-Lorenzo M., Engel A., Zäncker B., & Guieu C. Impact of dust enrichment on carbon budget and metabolism of Mediterranean plankton communities under present and future conditions of pH and temperature, in preparation (b) (this special issue)

53. Gitelson A., Karnieli, A., Goldman, N., Yacobi, Y.Z., & Mayo, M. (1996) Chlorophyll estimation in the Southeastern Mediterranean using CZCS images: adaptation of an algorithm and its validation, Journal of Marine Systems, 9, 283-290, doi:10.1016/S0924-7963(95)00047-X.

54. Gonzales, L., & Briottet, X (2017) North Africa and Saudi Arabia day/night sandstorm survey (NASCube), Remote Sensing, 9, 896, doi:10.3390/rs9090896.

55. Guerzoni, S., Chester, R., Dulac, F., Herut, B., Loÿe-Pilot, M. D., Measures, C., Migon, C., Molinaroli, E., Moulin, C., Rossini, P., Saydam, C., Soudine, A., & Ziveri, P. (1999) The role of atmospheric deposition in the biogeochemistry of the Mediterranean Sea, Progress in Oceanography, 44, 147-190, doi:10.1016/S0079-6611(99)00024-5.

56. Guerzoni, S., Quarantotto, G., Molinaroli, E., & Rampazzo, G. (1995) More data on source signature and seasonal fluxes to the Central Mediterranean Sea of aerosol dust originated in desert areas, in Water Poll. Res. Rep., 32, J.-M. Martin and H. Barth Eds., 253-260.

57. Guieu C., Aumont O., Gazeau F., Louis J., Ternon E., Leblond N., Bressac M., Contribution of the “lithogenic carbon pump” to POC export in the ocean, in preparation

58. Guieu C., Ridame, C., Pulido-Villena, E., Bressac, M., Desboeufs, K., & Dulac, F. (2014b) Impact of dust deposition on carbon budget: a tentative assessment from a mesocosm approach, Biogeosciences, 11, 5621-5635, doi:10.5194/bg-11-5621-2014.

59. Guieu, C., Aumont, O., Paytan, A., Bopp, L., Law, C.S., Mahowald, N., Achterberg, E.P., Marañón, E., Salihoglu, B., Crise, A., Wagener, T., Herut, B., Desboeufs, K., Kanakidou, M., Olgun, N., Peters, F., Pulido-Villena, E., Tovar-Sanchez, A,. & Völker, C. (2014a) The significance of episodicity in atmospheric deposition to Low Nutrient Low Chlorophyll regions, Global Biogeochemical Cycles, 2014, doi:10.1002/2014GB004852.

60. Guieu, C., Bonnet, S., Wagener, T., & Loÿe-Pilot, M.D. (2005) Biomass burning as a source of dissolved iron to open ocean? Geophysical Research Letters, 32, L19608, doi:10.1029/2005GL022962.

61. Guieu, C., Chester, R., Nimmo, M., Martin, J.M., Guerzoni, S., Nicolas, E., Mateu, J. & Keyse, S. (1997) Atmospheric input of dissolved and particulate metals to the northwestern Mediterranean, Deep-Sea Research II, 44, 655-674, doi: 10.1016/S0967-0645(97)88508-6.

62. Guieu, C., Loÿe-Pilot, M-D, Benyaya, L., & Dufour, A. (2010) Spatial and temporal variability of atmospheric fluxes of metals (Al, Fe, Cd, Zn and Pb) and phosphorus over the whole Mediterranean from a one-year monitoring experiment; Biogeochemical implications, Marine Chemistry, 120, 164-178, doi:10.1016/j.marchem.2009.02.004.

63. Heimbürger, L.E., Migon, C., Dufour, A., Chiffoleau, J.-F., & Cossa, D. (2010) Decadal trends and evolutions of trace-metals (Al, Cd, Co, Cu, Fe, Mn, Ni, Pb, Zn) in the western Mediterranean atmosphere, Science of the Total Environment, 408, 2629-2638, doi:10.1016/j.scitotenv.2010.02.042.

64. Holben, B.N., Eck, T.F., Slutsker, I., Tanré, D., Buis, J.P., Setzer, A., Vermote, E., Reagan, J.A., Kaufman, Y.J., Nakajima, T., Lavenu, F., Jankowiak, I., & Smirnov, A. (1998) AERONET—A federated instrument network and data archive for aerosol characterization, Remote Sensing of Environment, 66, 1-16, doi:10.1016/S0034-4257(98)00031-5.

65. Jacquet S, Garel M, Tamburini C, A. Dufour, N. Bhairy, S. Gasco & D. Lefèvre, Particulate biogenic barium and carbon remineralization fluxes at mesopelagic depths during the PEACETIME cruise, in preparation (this special issue)

66. Jordi, A., Basterretxea, G., Tovar-Sánchez, A., Alastuey, A., & Querol, X. (2012) Copper aerosols inhibit phytoplankton growth in the Mediterranean Sea, Proc. of the National Academy of Sciences, 109, 21246-21249, doi: 10.1073/pnas.1207567110.

67. Kallos, G., Spyrou, C., Astitha, M., Mitsakou, C., Solomos, S., Kushta, J., Pytharoulis, I., Katsafados, P., Mavromatidis, E., Papantoniou, N., & Vlastou, G. (2009) Ten-year operational dust forecasting - Recent model development and future plans. WMO/GEO Expert Meeting on an International Sand and Dust Storm Warning System, IOP Conference Series: Earth and Environmental Science, 7, 012012, doi:10.1088/1755-1307/7/1/012012.

68. Kanamitsu, M. (1989) Description of the NMC global data assimilation and forecast system, Weather and Forecasting, 4, 335-342, doi:10.1175/1520-0434(1989)004<0335:DOTNGD>2.0.CO;2.

69. Kouvarakis, G., Mihalopoulos, N., Tselepides, T., & Stavrakakis, S. (2001) On the importance of atmospheric nitrogen inputs on the productivity of eastern Mediterranean, Global Biogeochemical Cycles, 15, 805–818, doi:10.1029/2001GB001399.

70. Kubilay N., S. Nickovic, C. Moulin, & F. Dulac (2000) An illustration of the transport and deposition of mineral aerosol onto the eastern Mediterranean, Atmospheric Environment, 34, 1293-1303, doi:10.1016/S1352-2310(99)00179-X.

71. Law, C.S., Brévière E., de Leeuw, G., Garçon V., Guieu, C., Kieber, D.J., Kontradowitz, S., Paulmier, A., Quinn, P.K., Saltzman, E.S., Stefels, J., & von

Glasow, R. (2013) Evolving Research Directions in Surface Ocean-Lower Atmosphere (SOLAS) Science, Environmental Chemistry, 10, 1-16, doi:10.1071/EN12159.

72. Legrand, M., Plana-Fattori, A., & N'doumé, C. (2001) Satellite detection of dust using the IR imagery of Meteosat: 1. Infrared difference dust index, Journal of Geophysical Research: Atmospheres, 106, 18251-18274, doi:10.1029/2000JD900749.

73. Lionello P., Abrantes, F., Congedi, L., Dulac, F., Gacic, M., Gomiz, D., Goodess, C., Hoff, H., Kutiel, H., Luterbacher, J., Planton, S., Reale, M., Schröder, K., Struglia, M.V., Toreti, A., Tsimplis, M., Ulbrich, U., & Xoplaki, E. (2012) Introduction: Mediterranean climate−Background information, In The Climate of the Mediterranean Region: From the Past to the Future, P. Lionello Ed., Elsevier, pp. xxxv-xc, doi:10.1016/B978-0-12-416042-2.00012-4.

74. Louis J., Bressac, M., Pedrotti, M.L., & Guieu, C. (2015) Dissolved inorganic nitrogen and phosphorus dynamics in abiotic seawater following an artificial Saharan dust deposition, Frontiers in Marine Sciences, 2, 27, doi:10.3389/fmars.2015.00027.

75. Louis, J., Pedrotti, M. L., Gazeau, F., & Guieu, C. (2017) Experimental evidence of formation of Transparent Exopolymer Particles (TEP) and POC export provoked by dust addition under current and high $pCO_2$ conditions, PloS one, 12, e0171980, doi:10.1371/journal.pone.0171980.

76. Loÿe-Pilot, M. D., Martin, J. M., & Morelli, J. (1986) Influence of Saharan dust on the rain acidity and atmospheric input to the Mediterranean, Nature, 321, 427-428, doi:10.1038/321427a0.

77. Loÿe-Pilot, M.-D., & Martin, J.-M. (1996) Saharan dust input to the western Mediterranean: an eleven years record in Corsica, in The Impact of Desert Dust Across the Mediterranean, S. Guerzoni and R. Chester Eds., Kluwer, 191-199.

78. Mallet, M., Chami, M., Gentili, B., Sempéré, R., & Dubuisson, P. (2009) Impact of sea-surface dust radiative forcing on the oceanic primary production: A 1D modeling approach applied to the West African coastal waters. Geophysical Research Letters, 36, L15828, doi:10.1029/2009GL039053.

79. Mallet, M., et al. (2016) Overview of the Chemistry-Aerosol Mediterranean Experiment/Aerosol Direct Radiative Forcing on the Mediterranean Climate (ChArMEx/ADRIMED) summer 2013 campaign, Atmospheric Chemistry and Physics, 16, 455–504, doi:10.5194/acp-16-455-2016.

80. Marañón E, Pérez-Lorenzo M, Van Wambeke F, Uitz J, Dinasquet J, Haëntjens N, Dimier C, Deep maxima of phytoplankton biomass, primary production and bacterial production in the Mediterranean sea during late spring, in preparation (this special issue)

81. Marconi, M., Sferlazzo, D. M., Becagli, S., Bommarito, C., Calzolai, G., Chiari, M., di Sarra, A., Ghedini, C., Gómez-Amo, J. L., Lucarelli, F., Meloni, D., Monteleone, F., Nava, S., Pace, G., Piacentino, S., Rugi, F., Severi, M., Traversi, R., & Udisti, R. (2014) Saharan dust aerosol over the central Mediterranean Sea: $PM_{10}$ chemical composition and concentration versus optical columnar measurements, Atmospheric Chemistry and Physics, 14, 2039-2054, https://doi.org/10.5194/acp-14-2039-2014.

82. Markaki, Z., Loÿe-Pilot, M. D., Violaki, K., Benyahya, L., & Mihalopoulos, N. (2010) Variability of atmospheric deposition of dissolved nitrogen and phosphorus in the Mediterranean and possible link to the anomalous seawater N/P ratio, Marine Chemistry, 120, 187-194, doi:10.1016/j.marchem.2008.10.005.

83. Markaki, Z., Oikonomou, K., Kocak, M., Kouvarakis, G., Chaniotaki, A., Kubilay, N., & Mihalopoulos, N. (2003) Atmospheric deposition of inorganic phosphorus in the Levantine Basin, eastern Mediterranean: Spatial, temporal variability, and its role in seawater productivity, Limnology and Oceanography, 48, 1557–1568, doi:10.4319/lo.2003.48.4.1557.

84. Meloni, D., di Sarra, A., Biavati, G., DeLuisi, J.J., Monteleone, F., Pace, G., Piacentino, S., & Sferlazo, D.M. (2007) Seasonal behavior of Saharan dust events at the Mediterranean island of Lampedusa in the period 1999–2005, Atmospheric Environment, 41, 3041-3056, doi:10.1016/j.atmosenv.2006.12.001.

85. Menna, M., Poulain, P. M., Ciani, D., Doglioli, A., Notarstefano, G., Gerin, R., ... & Drago, A. (2019). New insights of the Sicily Channel and southern Tyrrhenian Sea variability. Water, 11(7), 1355.

86. Moon, J. Y., Lee, K., Tanhua, T., Kress, N., and Kim, I. N.: Temporal nutrient dynamics in the Mediterranean Sea in response to anthropogenic inputs, Geophysical Research Letters, 43, 5243–5251, doi:10.1002/2016GL068788, 2016.

87. Morales-Baquero, R., & Pérez-Martínez, C. (2016) Saharan versus local influence on atmospheric aerosol deposition in the southern Iberian Peninsula: Significance for N and P inputs, Global Biogeochemical Cycles, 30, 501-513, doi: 10.1002/2015GB005254.

88. Moulin, C., Lambert, C. E., Dayan, U., Masson, V., Ramonet, M., Bousquet, P., Legrand, M., Balkanski, Y.J., Guelle, W., Marticorena, B., Bergametti, G., & Dulac, F. (1998) Satellite climatology of African dust transport in the Mediterranean atmosphere. Journal of Geophysical Research: Atmospheres, 103, 13137-13144, doi:10.1029/98JD00171.

89. Moutin, T., Doglioli, A. M., De Verneil, A., & Bonnet, S. (2017) Preface: The Oligotrophy to the UlTra-oligotrophy PACific Experiment (OUTPACE cruise, 18 February to 3 April 2015), doi:10.5194/bg-14-3207-2017.

90. Nabat, P., Somot, S., Mallet, M., Michou, M., Sevault, F., Driouech F., Meloni, D., Di Sarra, A., Di Biagio, C., Formenti, P., Sicard, M., Léon, J.-F. and Bouin, M.-N. (2015), Dust aerosol radiative effects during summer 2012 simulated with a coupled regional aerosol-atmosphere-ocean model over the Mediterranean region, *Atm. Chem. Phys.*, 15, 3303-3326, doi:10.5194/acp-15-3303-2015.

91. Nencioli, F., d'Ovidio, F., Doglioli, A. M., & Petrenko, A. A. (2011) Surface coastal circulation patterns by in-situ detection of Lagrangian coherent structures, Geophysical Research Letters, 38, L17604, doi:10.1029/2011GL048815.

92. Pérez, C., Haustein, K. Janjic, Z. Jorba, O., Huneeus, N., Baldasano, J.M., Black, T., Basart, S., Nickovic, S., Miller, R.L., Perlwitz, J.P., Schulz, M., & Thomson, M. (2011) Atmospheric dust modeling from meso to global scales with the online NMMB/BSC-Dust model - Part 1: Model description, annual simulations and evaluation, Atmospheric Chemistry and Physics, 11, 13001-13027, doi:10.5194/acp-11-13001-2011.

93. Petrenko, A.A., Doglioli AM, Nencioli F., Kersalé M., Hu Z., & d'Ovidio F. (2017) A review of the LATEX project: mesoscale to submesoscale processes in a coastal environment, Ocean Dynamics, 67, 513-533, doi:10.1007/s10236-017-1040-9.

94. Pey, J., Querol, X., Alastuey, A., Forastiere, F., & Stafoggia, M. (2013) African dust outbreaks over the Mediterranean Basin during 2001–2011: $PM_{10}$ concentrations, phenomenology and trends, and its relation with synoptic and mesoscale meteorology. Atmospheric Chemistry and Physics, 13, 1395-1410, doi:10.5194/acp-13-1395-2013.

95. Pitta, P., Kanakidou, M., Mihalopoulos, N., Christodoulaki, S., Dimitriou, P. D., Frangoulis, C., Giannakourou, A., Kagiorgi, M., Lagaria, A., Nikolaou, P., Papageorgiou, N., Psarra, S., Santi, I, Tsapakis, M., Tsiola, A., Viollaki, K., & Petihakis, G. (2017) Saharan dust deposition effects on the microbial food web in the

Eastern Mediterranean: a study based on a mesocosm experiment. Frontiers in Marine Science, 4, 117, doi:10.3389/fmars.2017.00117.

96. Pulido-Villena E., A.-C. Baudoux, I. Obernosterer, M. Landa, J. Caparros, P. Catala, C. Georges, J. Harmand, & C. Guieu (2014) Microbial food web dynamics in response to a Saharan dust event: results from a mesocosm study in the oligotrophic Mediterranean Sea, Biogeosciences, 11, 5607–5619, doi:10.5194/bg-11-5607-2014.

97. Pulido-Villena, E., Van Wambeke, F., Desboeufs, K., Petrenko, A., Barrillon, S., Djaoudi, K., Doglioli, A., D'Ortenzio, F., Estournel, C., Fu, Y., Gaillard, T., Guasco, S., Marsaleix, P., Nunige, S., Raimbault, P., Taillandier, V., Triquet, S. & Guieu, C., Relative contribution of internal vs. external sources of phosphate to the surface mixed layer in the P-depleted Mediterranean Sea (Peacetime cruise), in preparation (this special issue)

98. Reygondeau, G., Irisson, J.-O., Ayata, S., Gasparini, S., Benedetti, F., Albouy, C., Hattab, T., Guieu, C., Koubbi, P. (2014) Definition of the Mediterranean eco-regions and maps of potential pressures in these eco-regions. Technical Report. Deliverable Nr. 1.6. FP7-PERSEUS project.

99. Richon, C., Dutay, J.-C., Dulac, F., Wang, R., & Balkanski, Y (2018b) Modeling the biogeochemical impact of atmospheric phosphate deposition from desert dust and combustion sources to the Mediterranean Sea, Biogeosciences, 15, 2499–2524, https://doi.org/10.5194/bg-15-2499-2018.

100. Richon, C., J.-C. Dutay, F. Dulac, R. Wang, Y. Balkanski, P. Nabat, O. Aumont, K. Desboeufs, B. Laurent, C. Guieu, P. Raimbault, & J. Beuvier (2018a) Modeling the impacts of atmospheric deposition of nitrogen and desert dust-derived phosphorus on nutrients and biological budgets of the Mediterranean Sea, Progress in Oceanography, 163, 21-39, doi:10.1016/j.pocean.2017.04.009.

101. Ridame C., Bigeard E., Dinasquet J., Tovar-Sanchez A., Baudoux A-C., Gazeau F. & Guieu C., Impact of dust enrichment on $N_2$ fixation and diversity of diazotrophs under present and future conditions of pH and temperature, in preparation (this special issue)

102. Ridame, C. , M. Le Moal, C. Guieu, E. Ternon, I. C. Biegala, S. L'Helguen, & M. Pujo-Pay (2011) Nutrient control of N2 fixation in the oligotrophic Mediterranean Sea and the impact of Saharan dust events, Biogeosciences, 8, 2773-2783, doi:10.5194/bg-8-2773-2011.

103. Ridame, C., Guieu, C. & S. L'Helguen (2013) Strong stimulation of $N_2$ fixation in oligotrophic Mediterranean Sea: results from dust addition in large in situ mesocosms, Biogeosciences, 10, 7333–7346, doi: 10.5194/bg-10-7333-2013.

104. Riffault V., C. Giorio, K. Desboeufs, J.-F. Doussin, F. Dulac, A. Féron, P. Formenti, F. Maisonneuve, E. Tison, S. Triquet, P. Zapf, Chemical characterization of gases and fine aerosols in air masses influenced by ship plumes during the PEACETIME cruise in the West Mediterranean basin, in preparation (this special issue)

105. Rolph, G., Stein, A., & Stunder, B. (2017) Real-time Environmental Applications and Display sYstem: READY, Environmental Modelling & Software, 95, 210-228, doi:10.1016/j.envsoft.2017.06.025.

106. Rousselet, L., Doglioli, A. M., de deVerneil, A., Pietri, A., Della Penna, A., Berline, L., Marrec, P., Grégori, G., Thyssen, M., Carlotti, F., Barrillon, S., Simon-Bot, F., Bonal, M., D'Ovidio, F., & Petrenko, A. (2019) Vertical motions and their effects on a biogeochemical tracer in a cyclonic structure finely observed in the Ligurian Sea, Journal of Geophysical Research: Oceans, 124, 3561-3574, doi: 10.1029/2018JC014392.

107. Roy-Barman M., Foliot L., Douville E., Guieu C., Leblond N., Gazeau F., Bressac M., Wagener T., & Ridame C., Contrasted release of insoluble elements (Fe, Al, REE, Th, Pa) during dust deposition in seawater: a minicosm approach, in preparation (this special issue)

108. Sciare, J., Bardouki, H., Moulin, C., & Mihalopoulos, N. (2003) Aerosol sources and their contribution to the chemical composition of aerosols in the Eastern Mediterranean Sea during summertime. Atmospheric Chemistry and Physics, 3, 291-302, doi:10.5194/acp-3-291-2003.

109. Seity, Y., Brousseau, P., Malardel, S., Hello, G., Bénard, P., Bouttier,F., Lac, C., and Masson, V.: The AROME-France Convective-Scale Operational Model, Mon. Weather Rev., 139, 976–991,https://doi.org/10.1175/2010MWR3425.1, 2011

110. Sellegri K., Nicosia A., Freney E., Uitz J., Thyssen M., Grégori G., , Engel A., Zäncker B., Haëntjens N., Mas S., Picard D., Saint-Macary A., Peltola M., Rose C., Trueblood J., Lefevre D., D'Anna B., Desboeufs K., Meskhidze N., Guieu C. and Law C., Linking living microorganisms of the Ocean and atmospheric Cloud Condensation Nuclei production, Science, submitted, 2020

111. SOLAS 2015-2025: Science Plan and Organisation (2015) SOLAS Scientific Steering Committee and Emilie Brévière (Editors) SOLAS International Project Office, Kiel. 68 pp.

112. Spyrou, C., Mitsakou, C., Kallos, G., Louka, P., & Vlastou, G. (2010) An improved limited area model for describing the dust cycle in the atmosphere, Journal of Geophysical Research: Atmospheres, 115, D17211, doi:10.1029/2009JD013682.

113. Stein, A.F., Draxler, R.R, Rolph, G.D., Stunder, B.J.B., Cohen, M.D., & Ngan, F. (2015) NOAA's HYSPLIT atmospheric transport and dispersion modeling system, Bull. Amer. Meteor. Soc., 96, 2059-2077, doi:10.1175/BAMS-D-14-00110.1.

114. Taillandier V., Prieur L. D'Ortenzio F., Ribera d'Alcalà M., and Pulido-Villena E., Profiling float observation of thermohaline staircases in the western Mediterranean Sea and impact on nutrient fluxes, Biogeosciences Discuss., https://doi.org/10.5194/bg-2019-504, 2020

115. Ternon E. , Guieu, C., Loÿe-Pilot, M-D., Leblond, N., Bosc, E., Gasser, B., Martin, J., & Miquel, J.-C. (2010) The impact of Saharan dust on the particulate export in the water column of the North Western Mediterranean Sea, Biogeosciences, 7, 809-826, doi: 10.5194/bg-7-809-2010.

116. Ternon E., Guieu, C., Ridame, C., L'Helguen, S, & Catala, P. (2011) Longitudinal variability of the biogeochemical role of Mediterranean aerosols in the Mediterranean Sea, Biogeosciences, 8, 1067–1080, doi: 10.5194/bg-8-1067-2011.

117. Testor P., Send, U., Gascard, J.-C., Millot, C., Taupier-Letage, I., & Béranger, K. (2005) The mean circulation of the southwestern Mediterranean Sea: Algerian Gyres, Journal of Geophysical Research, 110, C110017, doi:10.1029/2004JC002861.

118. The MERMEX Group (2011) Marine ecosystems' responses to climatic and anthropogenic forcings in the Mediterranean, Progress in Oceanography, 91, 97-166, doi:10.1016/j.pocean.2011.02.003.

119. Theodosi, C., Markaki, Z., Tselepides, A., & Mihalopoulos, N. (2010) The significance of atmospheric inputs of soluble and particulate major and trace metals to the eastern Mediterranean seawater, Marine Chemistry, 120, 154-163, doi: 10.1016/j.marchem.2010.02.003.

120. Thieuleux, F., Moulin, C., Bréon, F. M., Maignan, F., Poitou, J., & Tanré, D. (2005) Remote sensing of aerosols over the oceans using MSG/SEVIRI imagery, Annales Geophysicae, 23, 3561–3568, doi:10.5194/angeo-23-3561-2005.

121. Tovar-Sánchez A., A Rodríguez-Romero, A Engel, B Zäncker, F Fu, E Marañón, M Pérez-Lorenzo, M Bressac, T Wagener*, K Desboeuf, S Triquet, G Siour, C Guieu, Characterising the surface microlayer in the Mediterranean Sea: trace metals concentration and microbial plankton abundance, Biogeosciences Discuss., https://doi.org/10.5194/bg-2019-290, 2019

122. Tovar-Sánchez, A., Arrieta, J.M., Duarte, C.M., & Sañudo-Wilhelmy, S.A. (2014) Spatial gradients in trace metal concentrations in the surface microlayer of the Mediterranean Sea, Frontiers in Marine Science, 1, 79, doi: 10.3389/fmars.2014.00079.

123. Trueblood J., Nicosia, A., K. sellegri, E. Freney, B. Zäncker, A. Engel, D. Lefevre, M. Thyssen, G. Gregori, P. Amato, K. Desboeufs and C. Guieu, On the biological origin of the Ice Nuclei properties of primary marine emissions from the Mediterranean Sea, in preparation (this special issue)

124. Tsagaraki, T. M., Herut, B., Rahav, E., Berman Frank, I. R., Tsiola, A., Tsapakis, M.; Giannakourou, A., Gogou, A., Panagiotopoulos, C., Violaki, K.; et al. Atmospheric Deposition Effects on Plankton Communities in the Eastern Mediterranean: A Mesocosm Experimental Approach, Frontiers in Marine Science 2017, 4, 210. https://doi.org/10.3389/fmars.2017.00210.

125. Tsapakis, M., Apsotolaki, M., Eisenreich, S., & Stephanou, E.G. (2006) Atmospheric deposition and marine sedimentation fluxes of polycyclic aromatic hydrocarbons in the Eastern Mediterranean Basin. Environmental Science and Technology 40, 4922-4927.

126. Van Wambeke F., Pulido-Villena E., Djaoudi K., Garel M., Guasco S., Helias S., Dinasquet J., Tallandier V. & Tamburini C., Spatial patterns of biphasic ectoenzymatic kinetics in link with biogeochemical properties within surface, deep chlorophyll maximum layer, levantine intermediate waters and deep waters in the Mediterranean Sea in spring, in preparation (this special issue)

127. Varga, G., Újvári, G., & Kovács, J. (2014) Spatiotemporal patterns of Saharan dust outbreaks in the Mediterranean Basin, Aeolian Research, 15, 151-160, doi:10.1016/j.aeolia.2014.06.005.

128. Vincent, J., Laurent, B., Losno, R., Bon Nguyen, E., Roullet, P., Sauvage, S., Chevaillier, S., Coddeville, P., Ouboulmane, N., di Sarra, A. G., Tovar-Sánchez, A., Sferlazzo, D., Massanet, A., Triquet, S., Morales Baquero, R., Fornier, M., Coursier,

C., Desboeufs, K., Dulac, F., & Bergametti, G. (2016) Variability of mineral dust deposition in the western Mediterranean basin and south-east of France, Atmospheric Chemistry and Physics, 16, 8749-8766, doi:10.5194/acp-16-8749-2016.

129. Violaki K., Zarbas, P., & Mihalopoulos, N. (2010) Long-term measurements of water-soluble organic nitrogen (WSON) in atmospheric deposition in the Eastern Mediterranean: Fluxes, origin and biogeochemical implications, Marine Chemistry, 120, 179–186, doi:10.1016/j.marchem.2009.08.004.

130. Wagener, T., Guieu C., & Leblond N. (2010) Effects of dust deposition on iron cycle in the surface Mediterranean Sea: results from a mesocosm seeding experiment, Biogeosciences, 7, 3769-3781, doi: 10.5194/bg-7-3769-2010.

131. Wuttig K., Wagener, T., Bressac, M., Dammshäuser, A., Streu, P., Guieu, C., & Croot, P.L. (2013) Impacts of dust deposition on dissolved trace metal concentrations (Mn, Al and Fe) during a mesocosm experiment, Biogeosciences 10, 2583-2600, doi:10.5194/bg-10-2583-2013.

132. Yang, F., Pan, H.-L., Krueger, S.K., Moorthi, S., & Lord, S.J. (2006) Evaluation of the NCEP global forecast system at the ARM SGP site, Monthly Weather Review, 134, 3668-3690, doi:10.1175/MWR3264.1.

133. Zhang, J., Reid, J.S., Westphal, D.L., Baker, N.L., & Hyer, E.J. (2008) A system for operational aerosol optical depth data assimilation over global oceans, Journal of Geophysical Research: Atmospheres, 113, D10208, doi:10.1029/2007JD009065.

**Table 1.** Date of occupation, position and depth of the short stations (ST1-ST10), of the long stations (TYRR, ION, FAST) and of the SAV station.

| | arrival date | local time | departure date | local time | depth m | lat N | long E |
|---|---|---|---|---|---|---|---|
| ST1 | 12/05/2017 | 05:45 | 12/05/2017 | 21:15 | 1580 | 41°53.5 | 6°20 |
| ST2 | 13/05/2017 | 06:30 | 13/05/2017 | 13:08 | 2830 | 40°30.36 | 6°43.78 |
| ST3 | 14/05/2017 | 06:00 | 14/05/2017 | 13:30 | 1404 | 39°08.0 | 7°41.0 |
| ST4 | 15/05/2017 | 05:56 | 15/05/2017 | 13:04 | 2770 | 37°59.0 | 7°58.6 |
| ST5 | 16/05/2017 | 04:00 | 16/05/2017 | 10:58 | 2366 | 38°57.2 | 11°1.4 |
| TYRR | 17/05/2017 | 05:08 | 21/05/2017 | 15:59 | 3395 | 39°20.4 | 12°35.56 |
| ST6 | 22/05/2017 | 04:50 | 22/05/2017 | 10:38 | 2275 | 38°48.47 | 14°29.97 |
| SAV | 23/05/2017 | 11:30 | 23/05/2017 | 14:17 | 2945 | 37°50.4 | 17°36.4 |
| ST7 | 23/05/2017 | 21:10 | 24/05/2017 | 07:15 | 3627 | 36°39.5 | 18°09.3 |
| ION | 24/05/2017 | 18:02 | 29/05/2017 | 08:25 | 3054 | 35°29.1 | 19°47.77 |
| ST8 | 30/05/2017 | 03:53 | 30/05/2017 | 09:41 | 3314 | 36°12.6 | 16°37.5 |
| ST9 | 01/06/2017 | 19:13 | 02/06/2017 | 04:41 | 2837 | 38°08.1 | 5°50.5 |
| FAST | 02/06/2017 | 20:24 | 07/06/2017 | 23:25 | 2775 | 37°56.8 | 2°54.6 |
| ST10 | 08/06/2017 | 05:12 | 08/06/2017 | 10:25 | 2770 | 37°27.58 | 1°34.0 |
| FAST -bis | 08/06/2017 | 21:06 | 09/06/2017 | 00:16 | 2775 | 37°56.8 | 2°55.0 |

**Table 2. Work at sea during the PEACETIME Cruise and associated publications**

| total number | Operations at sea | details | SHORT STATIONS | | | | | | | | | | | LONG STATIONS | | | Papers presenting the data |
|---|---|---|---|---|---|---|---|---|---|---|---|---|---|---|---|---|---|
| | | | 1 | 2 | 3 | 4 | 5 | 6 | 7 | 8 | 9 | 10 | SAV | TYR | ION | FAST | |
| continuous | Atmospheric sampling | [1] | CONTINUOUS | | | | | | | | | | | | | | Desboeufs et al., in prep (a), Desboeufs et al., in prep (b); Fu et al., in prep. (a); Garcia-Nieto et al., in prep.; Riffault et al., in prep. |
| 3 | Rain water collection | [2] | | | | | | | | | | | | | x | x | Fu et al., in prep (b) |
| continuous | Continuous surface seawater pumping (-5 m) | [3] | CONTINUOUS | | | | | | | | | | | | | | Freney et al., in prep.; Sellegri et al., submitted; Trueblood et al., in prep. |
| 3 times | Surface seawater pumping (large volume (1800 L) for experiments in Climate Reactors) | [4] | | | | | | | | | | | | x | x | x | Gazeau et al., in prep (a & b); Ridame et al., in prep.; Roy-Barman et al., in prep.; Dinasquet et al., in prep.; Guieu et al., in prep. |
| 90 casts | Classical Rosette with 24 Niskin bottles or 22 Niskin bottles + 3 HP bottles [1]. | [5] | 0-500 and 0-bottom | | | | | | | | | | | | | | Taillandier et al., submitted; van Wambeke et al., in prep.; Maranon et al., in prep.; Berline et al., in prep.; Jacquet et al., in prep.; Zancker et al., in prep.; Barbieux et al., in prep.; Baumas et al., in prep. Guieu et al., this paper ; Garel et al., 2019 |
| 27 casts | Trace metal Clean Rosette on kevlar cable with 24 teflon-coated GoFlo bottles [2]. | [6] | 0-bottom | | | | | | | | | | | | | | Bressac et al., in prep.; Pulido-Villena et al., in prep.; Desgranges et al., in prep., Ridame et al., in prep. |
| 17 sampling | Microlayer sampling (rubber boat) | [7] | x | | x | x | x | x | x | x | x | | x | xx | xx | xxxx | Tovar-Sanchez et al., in rev.; Zancker et al., in prep.; Engel et al., in prep. |
| 17 free-fall profiles | Optical measurements: HyperPro [3] | [8] | x | x | x | x | x | x | | | | | x | xxxx | xx | xxxx | |
| 23 net tows | Zooplankton Net (0-200 m) | [9] | x | x | x | x | x | x | x | x | x | | | xxxx | xxxxx | xxxxx | Feliu et al., in prep. |
| 13 | Marine snow catcher (depth m) | [10] | | | | | | | | | | | | 70 -80 -90 - 200 | 80 -100 - 150 - 200 | 70 -75 - 80- 100 | |

*Table 2 (continued)*

| | | | | | | | | | | | | | | | | | |
|---|---|---|---|---|---|---|---|---|---|---|---|---|---|---|---|---|---|
| 3 times | Drifting mooring | [11] | | | | | | | | | | | | x | x | x | Bressac et al., (2019); Bressac et al., in prep. |
| 3 times | Sediment Cores | [12] | | | | | | | | | | | | x | x | x | Brandt et al., submitted; Brandt et al., in prep. |
| 20 drifters | SVP (Surface Velocity Program) drifters | [13] | | | | | | | | | | | | x | x | | Menna et al., 2019. Guieu et al., this paper; Berline et al.in prep., Desboeufs et al., in prep. (b) |
| a total of 1000 profiles (0-300m) | Moving Vessel Profiler (begining and end long stations) | [14] | between the short stations and in the long stations area as frequent as possible | | | | | | | | | | | | | | Guieu et al., this paper; Berline et al. in prep. |
| 2 deployments, 1 recovery | Biogeochemical ARGO float | [15] | | | | | | | | | | | x | | x | | Barbieux et al., in prep. ; Taillandier et al., submitted |

1] Atmospheric sampling was carried out throughout the transect using PEGASUS dedicated mobile platform (PortablE Gas and Aerosol Sampling UnitS, Formenti et al., 2019) to monitor continuous air gaseous composition (NOx, $SO_2$, $O_3$, $CO_2$, CO, VOC), physico-chemical properties of aerosol particles (mass and number concentration, size-distribution, chemical composition and nutrients contents), parameters of atmospheric dynamics such as the boundary layer, and radiative parameters (incident radiation, optical thickness, optical properties of the particles).

[2] Rain sampling of two events that occurred during the cruise. The on-line filtration collector was used to determine the dissolved and particulate composition of rain, including major and trace metals (Al, Ba, Cd, Co, Cr, Cu, Fe, Mo, Mn, Ni, Pb, Sr, Ti, V, Zn), atmospheric inorganic compounds (sulfate, chlorure, Na, Mg, K, Ca,.. ) and dissolved nutrients (phosphate, nitrate, ammonium).

[3] An innovative system of continuous "clean" pumping activated by a large peristaltic pump connected to a tube plunged at 5 m under the surface seawater inside a TraOcean was set up. The water was conveyed in a dedicated laboratory and distributed to several instruments to assess its

chemical properties (carbonate chemistry, $O_2$), microbial assemblages, hydrological properties, optical properties related to community and particle composition and aerosol production (chemical composition, particles spectrum) throughout the transect.

[4] Climate reactor experiments: 6 large volume tanks (300 L) were filled with surface water. After artificial dust seeding at the surface of 4 of the reactors, the impact of dust deposition on biogeochemical stocks and fluxes under present and future environmental conditions (acidification and increase of the temperature of the sea water) was followed during 4 days (TYR and ION) and 5 days (FAST). [listing all parameters measured: see Table 1, Gazeau et al., this issue (a)].

[5] The ”classical” Rosette was composed of a CTD underwater unit that continuously collected the following parameters: pressure, temperature and salinity of seawater, dissolved oxygen concentration, photosynthetically active radiation (PAR), beam transmission (at 650 nm), chlorophyll-a fluorescence. A LISST (Laser *in situ* Scattering and Transmissiometry Deep (LISST-Deep), Sequoia Sc) was mounted independently on the CTD frame. This instrumental package was also composed of a sampling system : 24 12-L Niskin bottles could be fired at specified levels during upcasts. Some Niskin could be replaced by High Pressure (HP) bottles that allowed hyperbaric sampling on dedicated deep casts. Water from the classical Rosette was used to quantify $O_2$, AT/CT, nutrients, DOC, POC/PON, hyperspectral particulate absorption coefficient, hyperspectral CDOM absorption coefficient, chlorophyll pigments, viruses abundance and lysogeny, bacteria, flagellates and pico-nanoeukaryotes abundance (by cytometry), total combined carbohydrates, total hydrolysable amino acids, gel particles (TEP and CSP), bacterial production, dissolved and particulate primary production, virus diversity, and eukaryote diversity.

[6] The trace metal “clean” Rosette was composed of a titanium CTD underwater unit that continuously collected the following parameters: pressure, temperature and salinity of seawater, dissolved oxygen concentration, CDOM Fluorescence. This instrumental package was also composed of a teflon-coated sampling system: 24 GoFlo bottles could be fired at specified levels during upcast. Water from the clean rosette was used to measure dissolved metals (Al, Cd, Co, Cu, Fe, Mo, Ni, Pb, V, Zn) and particulate (Al, Ba, Ca, Cu, Fe, Mn, Ni, Ti, Zn), total mercury, methyl mercury, inorganic phosphate and nitrate (nano-molar), nutrients (to be measured with Technicon), di-nitrogen fixation, diazotrophs diversity (only at Station 10).

[7] Discrete sampling of the surface micro layer (SML) was performed from a rubber boat using gas plate systems. Dissolved (<0.22 µm) and total (unfiltered) SML samples were collected for trace metals (Cd, Co, Cu, Fe, Ni, Mo, V, Zn and Pb) and nutrients analysis. Same metals were also measured in a subsurface (0-1 m) filtered (0.22 µm) sample. Samples were collected for the determination of total combined carbohydrates, total hydrolysable amino acids, gel particles (TEP and CSP). DNA was extracted from filters from the surface microlayer and subsurface water (~ 20 cm). Three experimental SML additions were carried out in waters of TYR, ION and FAST stations.

[8] The HyperPro measured hyperspectral upwelling radiance (Lu) and downwelling irradiance (Ed) at the daily solar maximum.

[9] Samples collected by net hauls between 0 and 300 m performed with a BONGA net equipped with a 100 µm and a 200 µm mesh size. Zooplankton abundance, biomass and taxonomy were obtained in 3 size classes: <200 µm; >200 - <1000 µm and >1000 µm. At long stations, additional samples were taken for stable isotopes analyses.

[10] The large Marine Snow Catcher bottle (100 L) was used at long duration stations to collect suspended particles, slow sinking particles and fast sinking particles. Heterotrophic production of prokaryotes attached to these different particles types was measured along with TEP abundance and POC concentrations. In addition concentration kinetics of aminopeptidase, alkaline phosphatase and beta D glucosidase was measured. Diversity of microorganisms collected in each type of particles was analyzed by barcoding and sequencing.

[11] The mooring was equipped with (i) 3 Technicap type PPS5 particle traps at 200, 500 and 1000 m, each equipped with inclinometers, (ii) 3 IODA (In Situ Oxygen Dynamics Auto-analyzer) at 5, 90 and 200 m; (iii) 2 in situ particle interceptor/incubator – RESPIRE (at 120 m and 200 m), (iv) 2 trace metal clean RESPIRE (at 110 m and 190 m), and (v) 1 Sediment Trap Station with 4, ø80-mm tubes in transparent PVC. The line was also equipped with 4 CTD / O2 type SeaBird Microcat SBE37, 4 Aquadopp Doppler current meter from Nortek brand, 5 RBR Autonomous Temperature and Pressure Sensors, 5 RBR Autonomous Temperature Sensors alone. Drifting moorings were deployed for 4 days at TYR and ION and 5 days at FAST. Fluxes for particulate mass, carbon, organic carbon, inorganic carbon, nitrogen, calcium, aluminium, iron, biogenic and lithogenic silica were determined from PPS5 samples.

[12] At TYR (depth 3395 m), ION (depth 3054 m) and FAST (2775 m), sediment core sampling were carried out with a multicorer, sliced into depth layers to perform DNA extractions.

[13] A total of 20 SVP (Surface Velocity Program) drifters were deployed at the long duration stations to provide information on the current at 15-m depth.

[14] A MVP (Moving Vessel Profiler) was deployed to perform high frequency 0-300 m profiles of CTD (and fluorescence and LOPC-Laser Optical Particle Counter, when the “big fish” was towed instead of the “small fish”) between the short stations and in the long station areas as frequently as possible (see Figure 12). A total of more than 1000 profiles have been obtained.

[15] Two Biogeochemical Argo profiling floats have been deployed in the Ionian Sea. In addition to the CTD, the floats interfaced bio-optical sensors that measured fluorescence of Chlorophyll and CDOM, particulate backscattering (700 nm), Photosynthetically Active Radiation and downwelling irradiance at three wavelengths (380, 412, 490 nm). In addition, the float released at the ION station included an optode that measures dissolved oxygen and a beam transmissometer (650 nm).

**Figure Captions.**

**Figure 1**. Mediterranean surface mixed layer depth (m) monthly climatology over 1940-2004 (in m; from D'Ortenzio et al., 2005; Copyright 2005 by the American Geophysical Union).

**Figure 2**. Monthly-averaged dust optical depth at 550 nm (1979-2013 period) over the Mediterranean region from the CNRM-RCSM5 regional coupled climate system model (after Nabat et al., 2015).

**Figure 3**. Monthly averaged chlorophyll maps derived from SeaWiFS data for the year 1999 (Bosc et al., 2004; Copyright 2004 by the American Geophysical Union).

**Figure 4.** Spatial distribution of the Mediterranean epipelagic marine ecosystems of the Mediterranean Sea (from Reygondeau et al. 2014). The consensus regions (in white, from Ayata et al., 2018) from eight regionalisations of the Mediterranean Sea, are characterised by well defined, relatively homogeneous biogeochemical and hydrodynamical conditions, with similar temporal dynamics). The transect initially planned is superimposed.

**Figure 5**. Transect of the PEACETIME Cruise: Initial (dotted line) and final track (continuous line); stations are indicated by filled circles (planned stations: smaller, pink: realized: larger, orange). The 10 short stations are numbered from St.1 to St.10. TYR, ION, and FAST indicate the 3 long stations. The SAV station was only performed for the retrieval and launch of floats. The land-based Lampedusa observatory (purple triangle) and 15 AERONET stations operated during the cruise are also represented (brown diamonds).

**Figure 6**. Aerosol optical depth at 550 nm derived from MSG/SEVIRI on 3 June 2017; left: from the 15-mn image acquired at 13:00 UT; right: daily average from 52 images acquired between 4 and 18:30 UT. The black circle indicates the position of the ship (station FAST) .

The dark grey mask corresponds to land and coastal ocean pixels, the light grey, to cloudy pixels.

**Figure 7.** NASCube image window over North Africa and southern Europe for 1 June 2017, 02 UT. This nighttime image is derived from MSG/SEVIRI thermal infrared channels by comparison to a clear reference image for the period, allowing detecting high dust load over the continental surfaces (Legrand et al., 2001). White tones indicate clouds, the highest being the brightest and the thermal anomalies attributable to dust are coloured by increasing intensity from blue to pink. They are associated with increasing AOD from light blue (typically <0.3) to purple (~1) and pink (>2) (Gonzalez and Briottet, 2017).

**Figure 8.** Rain-lightning-clouds (RLC) image window over the western Mediterranean and Spanish Peninsula showing clouds (white areas), estimated precipitation (blue shades), and lightning strikes (yellow circles) obtained by combining SEVIRI infrared images and European rain radars (from meteoradar.co.uk; access 3 June 2017).

**Figure 9.** Maps of 6-h accumulated desert dust wet deposition fluxes in the western Mediterranean produced by the forecast run of 2 June 2017 of the three dust transport models NNMB-BSC-Dust-v2 (top) BSC-DREAM8b (middle) and SKIRON (bottom), ~~at times 3 Jun, 12 UTC and 18 UTC, 4 Jun 18 UTC and 5 Jun 00 UTC, from left to right, respectively.~~

**Figure 10.** Map of the FSLE (Finite Size Lyapunov ~~Exposant~~, ~~day$^{-1}$~~) calculated from the near-real-time altimetry-derived surface currents for June 4, 2017. The figure is taken from the SPASSO bulletin of June 5, 2017 with the planned stations shown in black and the route toward the FAST station highlighted in magenta.

**Figure 11.** (1) Rain rate (mm h$^{-1}$) during the night between the 4$^{th}$ and 5$^{th}$ of June (white dot is the position of the FAST station). These European radar composite products were provided by

the Odyssey system, created in the framework of the Opera Program ~~that is~~ the radar component of the Eumetnet observation Program.

**Figure 12.** MVP measurements across the FAST station. In the upper panel, the positions of each MVP cast ~~(~~and ~~of the~~ FAST station~~)~~ are shown as black ~~(~~and red~~)~~ crosses. ~~Below~~ are show~~n~~ the ~~sections of~~ temperature (top), salinity (middle) and density (bottom).

The map of the altimetry derived currents shows clearly the presence of the Algerian eddy west to the FAST station sampled during the MVP transect (figure 13).

**Figure 13.** Geostrophic currents from satellite data with the Ekman component from WRF model added (black arrows, ~~mean during the shown transect~~). In addition, in situ drifter trajectories during 30 days (launched at FAST and in its vicinity) are ~~re~~presented as white lines. Horizontal currents measured by the VM-ADCP for the first two bins (purple arrows -18 m, salmon arrows -26 m) are superimposed for comparison.

**Figure 14.** ARIANE particles initial positions (white) and after a backward integration of 1 (pink), 2 (light red), 3 (dark red), and 10 days (black) for the FAST station on the 3rd of June. (a) large view, (b) zoomed view, (c) ratio of particles remaining in the initial zone as a function of the number of backward integration days.

**Figure 15.** Left panels: temperature-salinity diagram (upper ~~panel~~), temperature profiles (middle ~~panels~~), and ~~profiles of~~ beam transmission (lower ~~panel~~). Right panels: evolution of the surface stratification ($s_q$, upper ~~panel~~), salinity ~~(~~anomalies ~~to the profile of $t_0$ –~~ 2nd June 16h30~~, middle~~ panel) and chlorophyll fluorescence (lower ~~panel~~) at the FAST station. Time ~~Series are composed of 43 repeated CTD casts, with variable temporal resolution~~. The depth of the mixed layer is indicated by white dots. The time of the rainfall is indicated by the red line.

**Figures 16.** Sea Surface Temperature during ~~the cruise~~; left) ~~outward route (~~10-28 May), right) ~~return route (~~28 May-~~10~~ June). ~~The daily satellite pixel data are used to produce a~~ weighted mean. The weight for each pixel ~~is~~ calculated ~~by normalizing by~~ the square of the inverse distance from the pixel to the daily mean ship position. The ship track is shown in black, ~~the~~ short ~~(long)~~ station positions are indicated with black dots ~~(~~squares~~)~~. Data courtesy of L.Rousselet.

**Figure 17.** As figure ~~17~~, ~~but for the~~ satellite-derived surface Chlorophyll-a concentration ~~averaged over the entire duration of the cruise~~. Data courtesy of L.Rousselet.

~~**Figure 18.** Nitrate (top right) and phosphate (bottom right; see Pulido-Villena et al., in prep.) concentrations (in nM) above 100 m,~~ during ~~the~~ PEACETIME ~~cruise along the west-east gradient shown on the map (left).~~

**Figures**

**FIG 1**

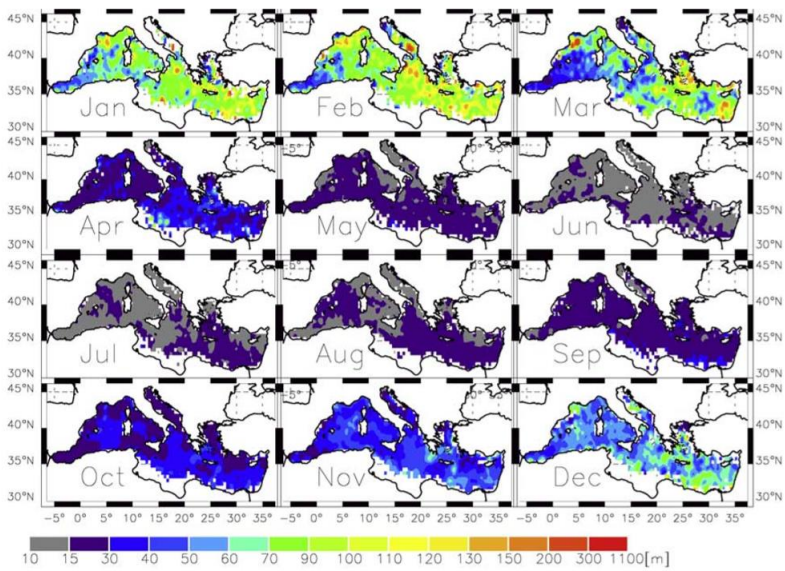

**FIG 2**

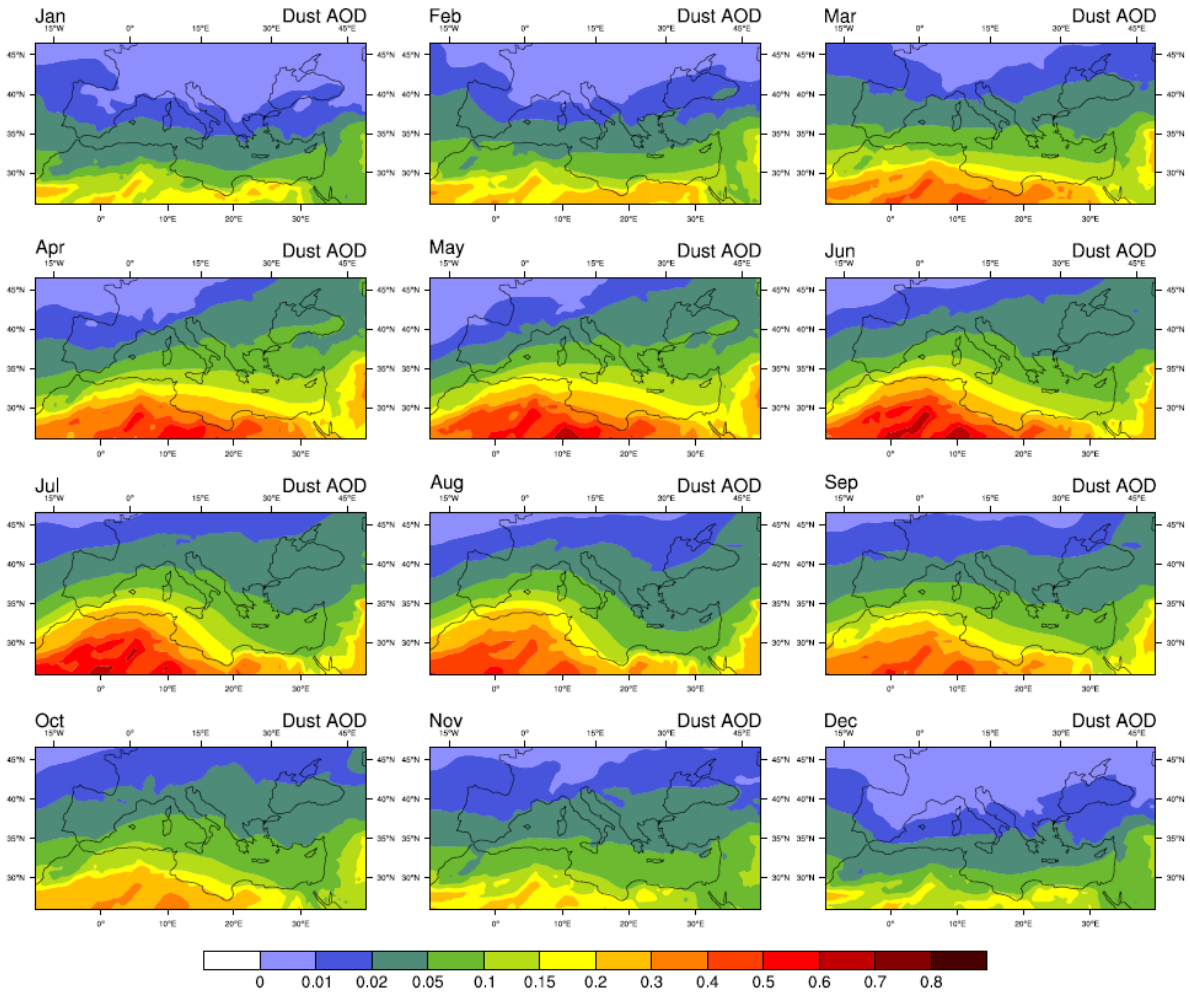
Jan
Dust AOD
Feb
Dust AOD
Mar
Dust AOD
Apr
Dust AOD
May
Dust AOD
Jun
Dust AOD
Jul
Dust AOD
Aug
Dust AOD
Sep
Dust AOD
Oct
Dust AOD
Nov
Dust AOD
Dec
Dust AOD
0
0.01
0.02
0.05
0.1
0.15
0.2
0.3
0.4
0.5
0.6
0.7
0.8

**FIG 3**

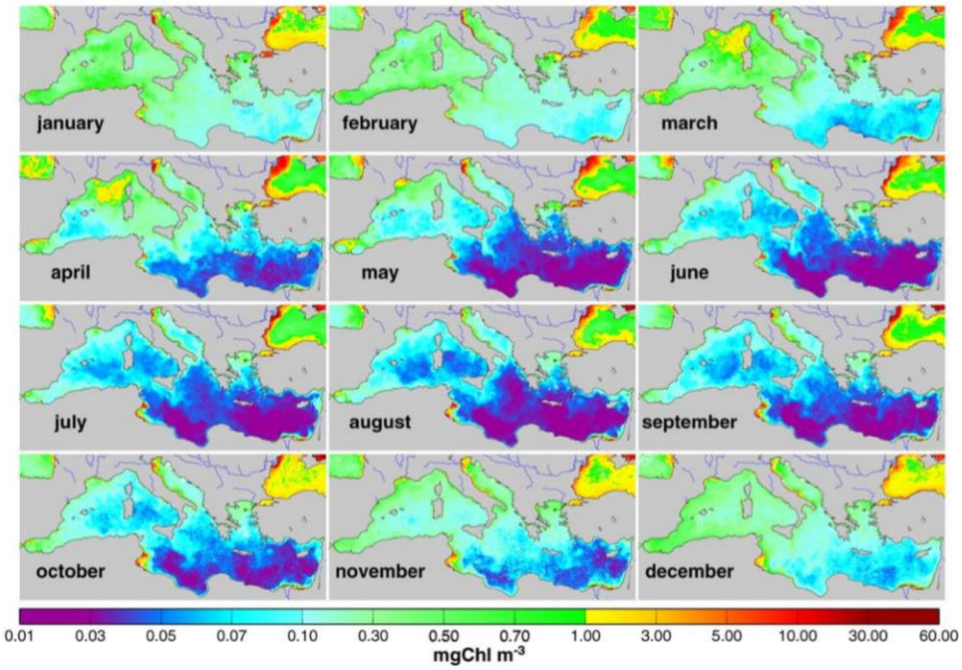
january
february
march
april
may
june
july
august
september
october
november
december
0.01
0.03
0.05
0.07
0.10
0.30
0.50
0.70
1.00
3.00
5.00
10.00
30.00
60.00
mgChl m-3

**FIG 4**

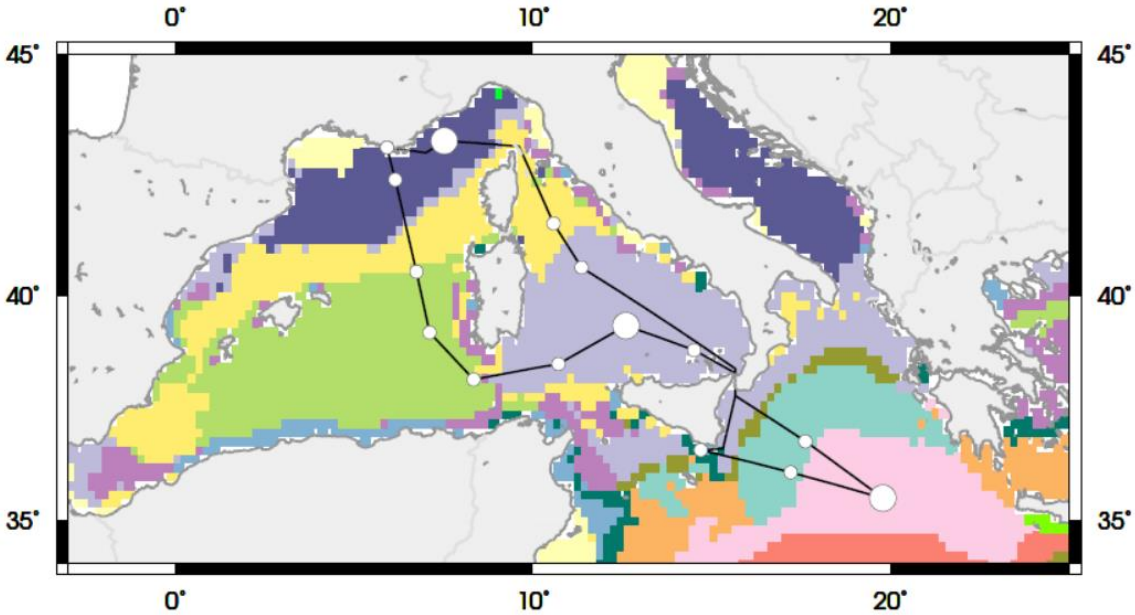
0°
10°
20°
45°
40°
35°

**FIG 5**

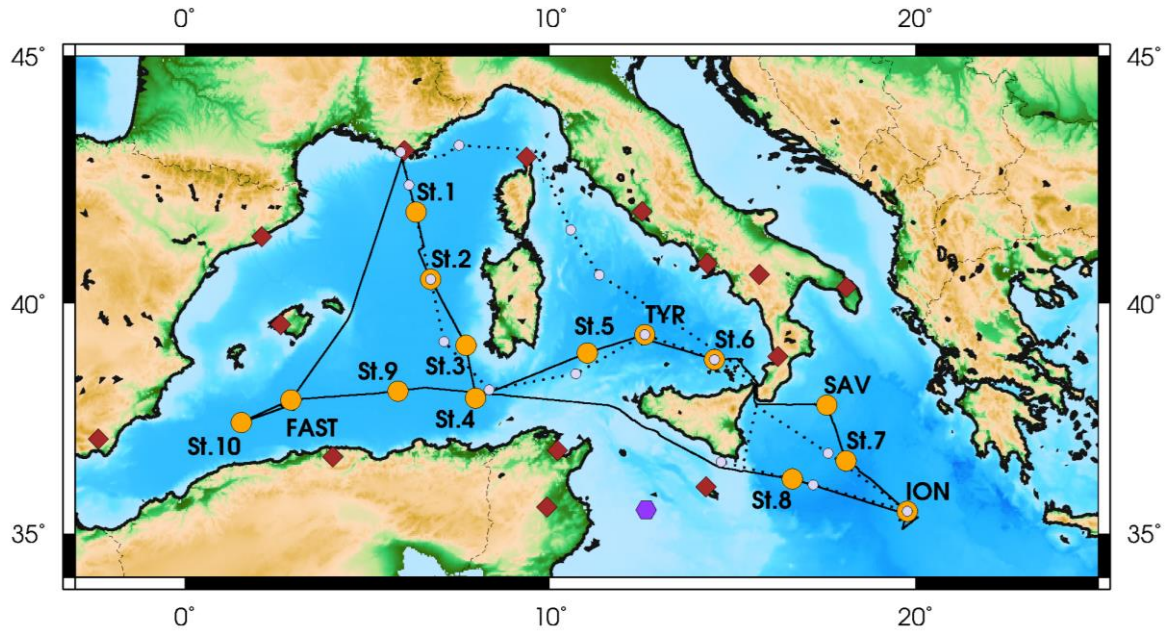
0°
10°
20°
45°
40°
35°
St.1
St.2
St.3
St.4
St.5
TYR
St.6
St.7
St.8
St.9
St.10
FAST
SAV
ION

**FIG 6**

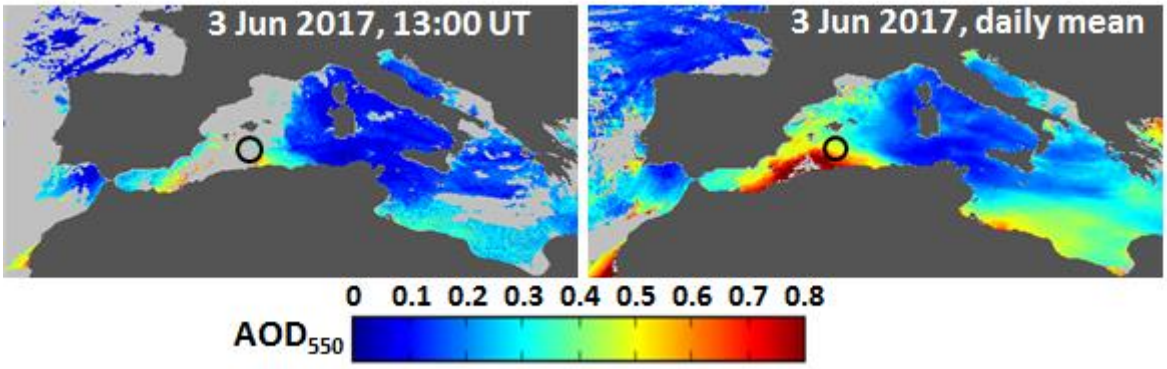
3 Jun 2017, 13:00 UT
3 Jun 2017, daily mean
0 0.1 0.2 0.3 0.4 0.5 0.6 0.7 0.8
AOD550

**FIG 7**


1 Jun 2017, 02:00 UT

**FIG 8**

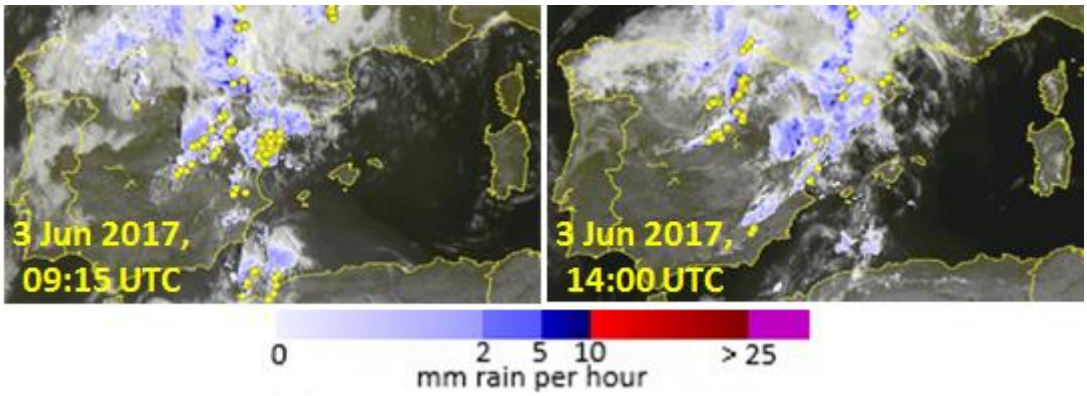
3 Jun 2017,
09:15 UTC
3 Jun 2017,
14:00 UTC
0
2
5
10
> 25
mm rain per hour

**FIG 9**

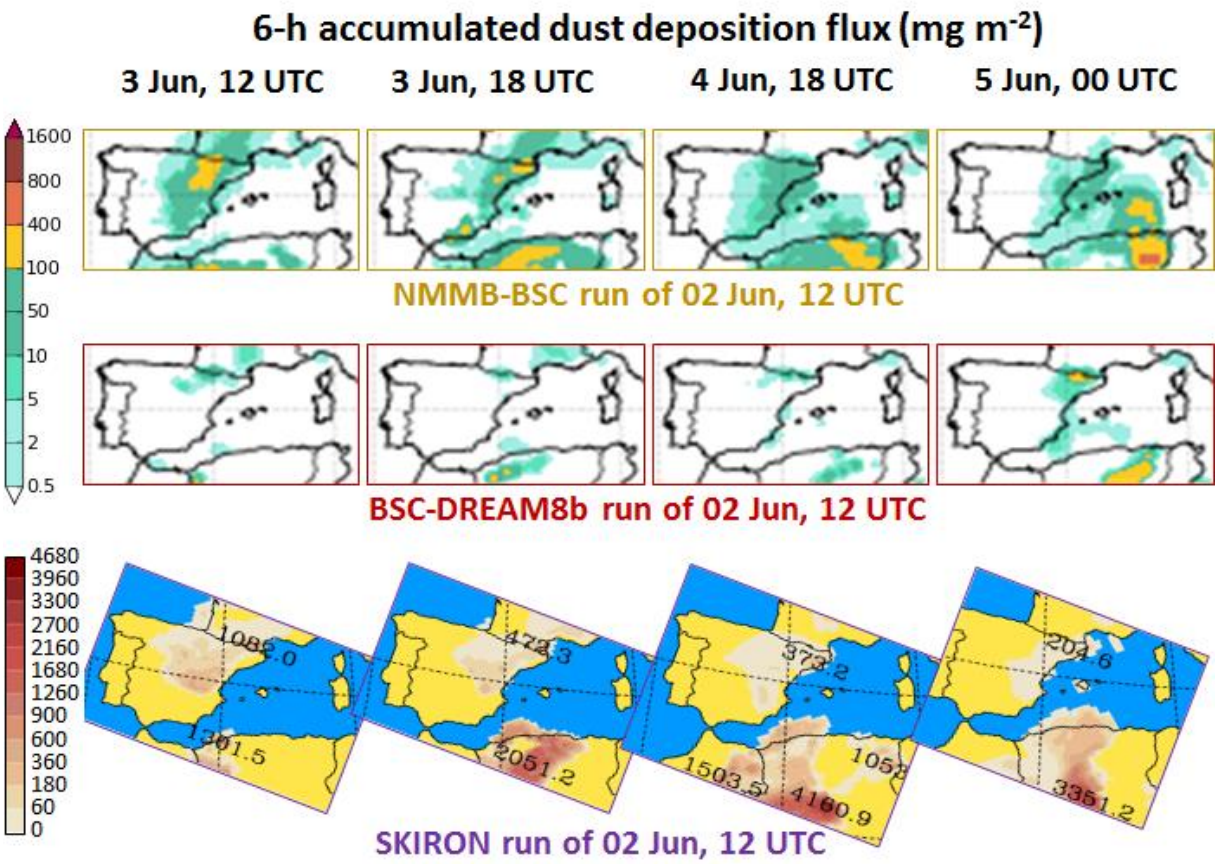
6-h accumulated dust deposition flux (mg m-2)
3 Jun, 12 UTC
3 Jun, 18 UTC
4 Jun, 18 UTC
5 Jun, 00 UTC
1600
800
400
100
50
10
5
2
0.5
NMMB-BSC run of 02 Jun, 12 UTC
BSC-DREAM8b run of 02 Jun, 12 UTC
4680
3960
3300
2700
2160
1680
1260
900
600
360
180
60
0
1086.0
1301.5
4723.3
2051.2
3732
1503.5
4160.9
204.6
3351.2
SKIRON run of 02 Jun, 12 UTC

**FIG 10**

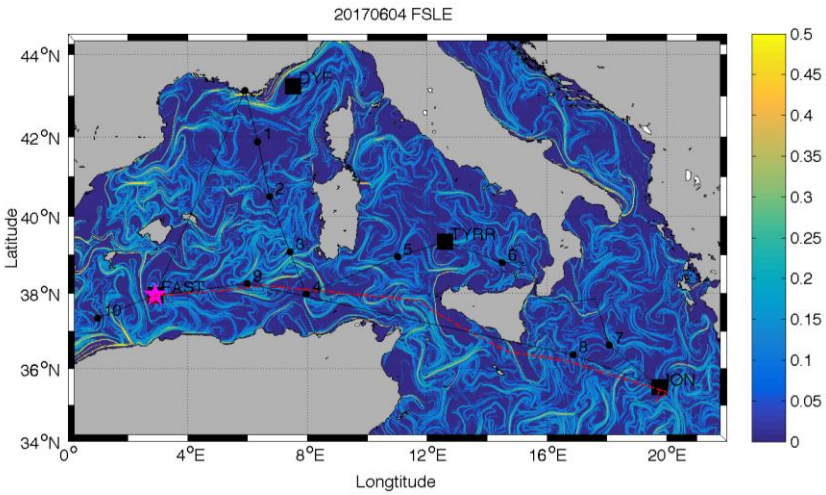
20170604 FSLE
44°N
42°N
40°N
38°N
36°N
34°N
Latitude
0°
4°E
8°E
12°E
16°E
20°E
Longtitude
PYR
TYRR
EAST
ION
0.5
0.45
0.4
0.35
0.3
0.25
0.2
0.15
0.1
0.05
0

**FIG 11**

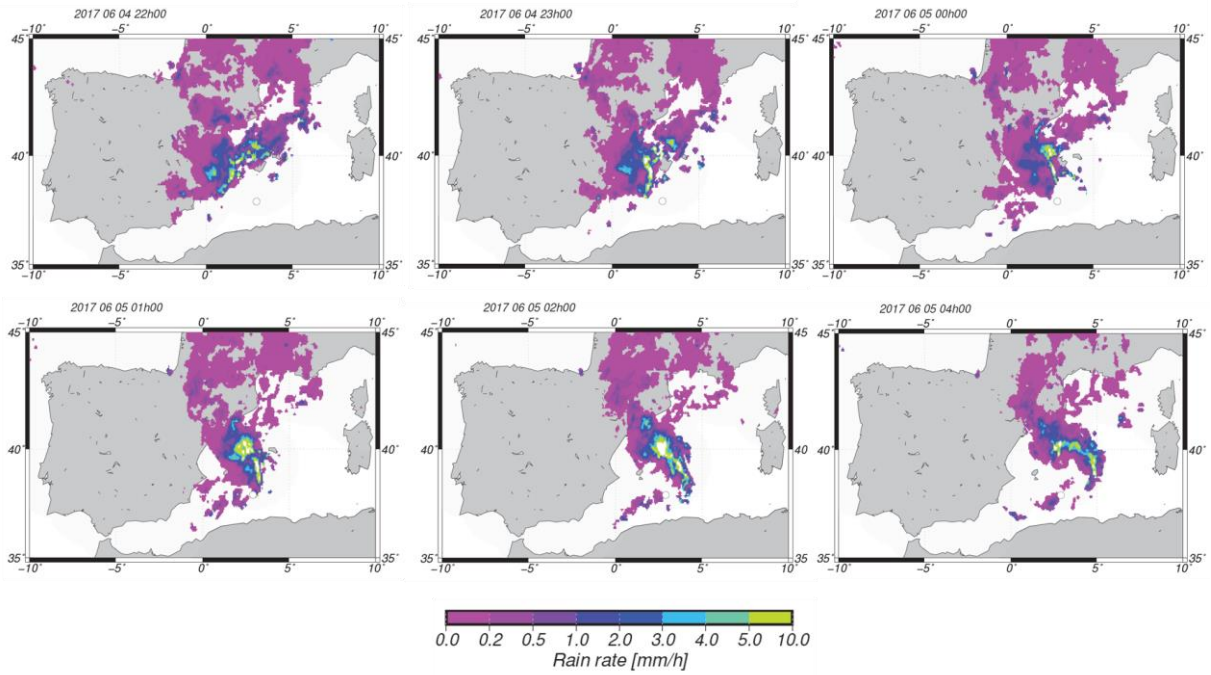
2017 06 04 22h00
2017 06 04 23h00
2017 06 05 00h00
2017 06 05 01h00
2017 06 05 02h00
2017 06 05 04h00
0.0 0.2 0.5 1.0 2.0 3.0 4.0 5.0 10.0
Rain rate [mm/h]

**FIG 12**

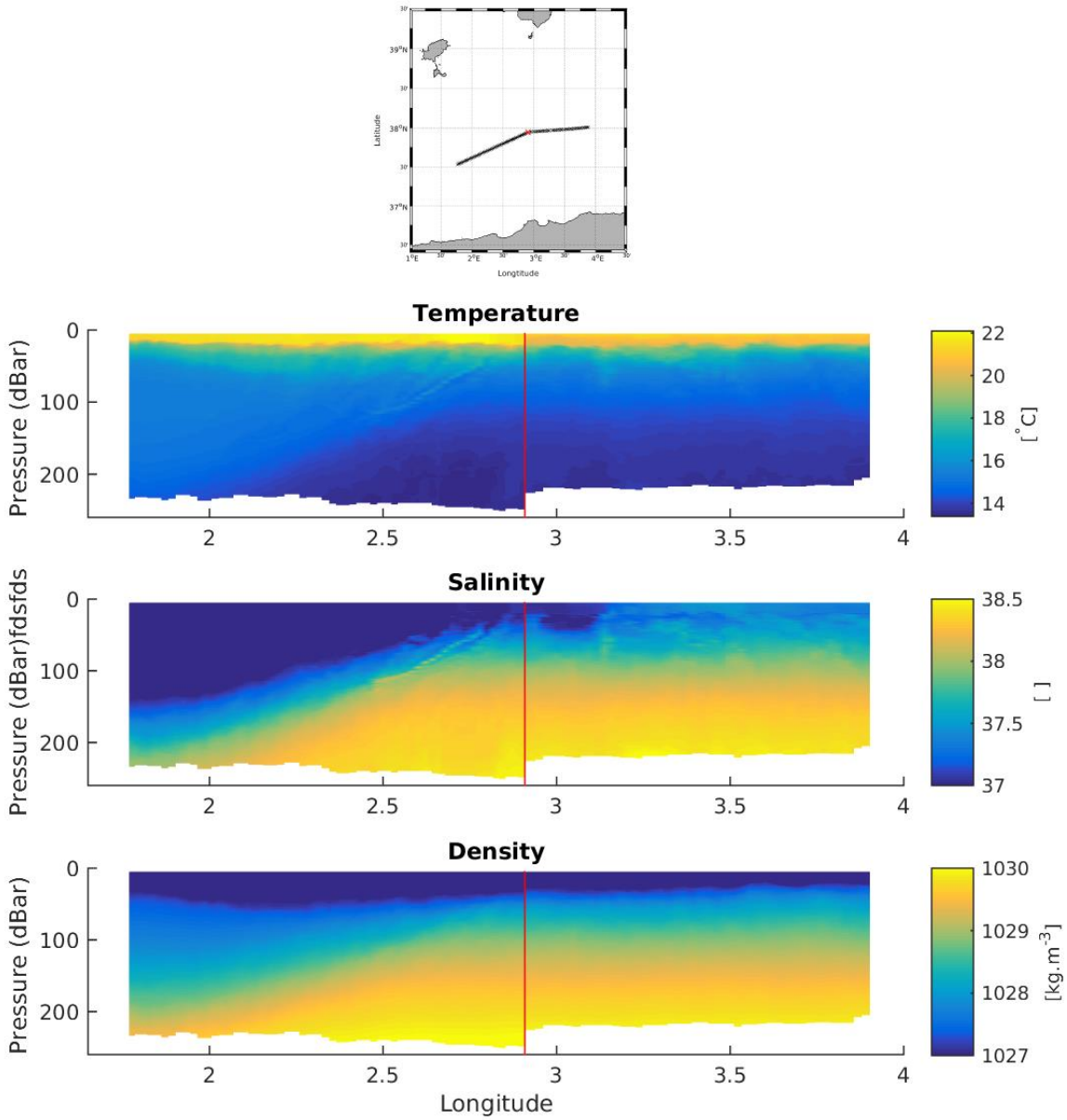
Latitude
Longtitude
Temperature
Pressure (dBar)
[°C]
Salinity
Pressure (dBar)fdsfds
[ ]
Density
Pressure (dBar)
[kg.m-3]
Longitude

**FIG 13**

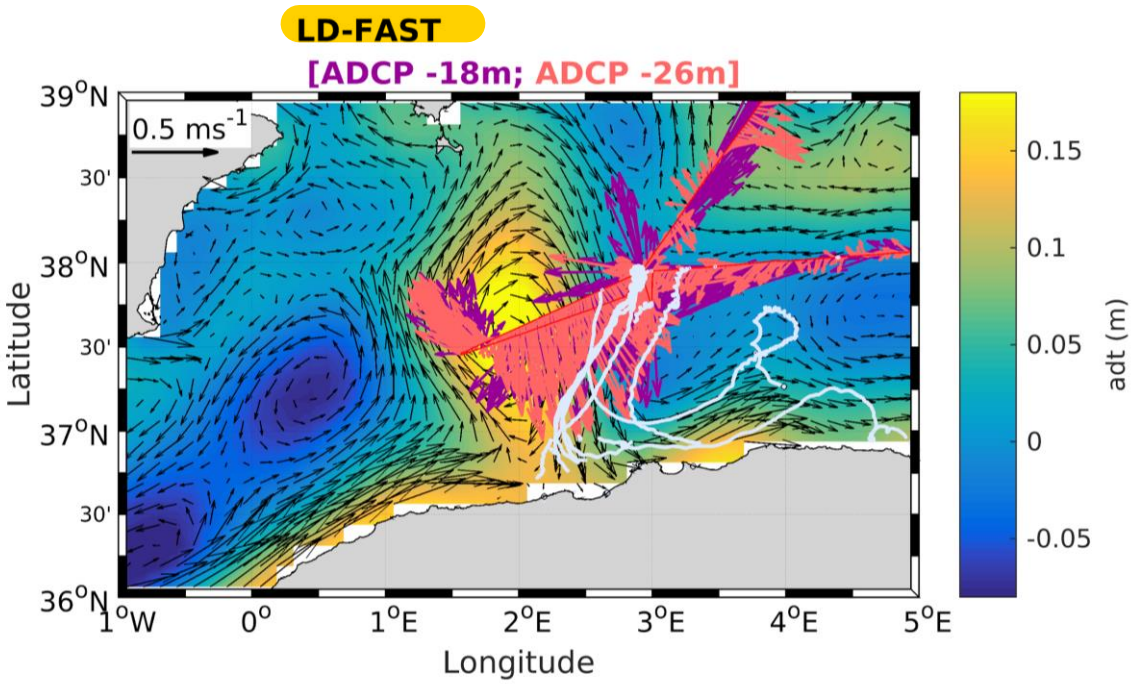
LD-FAST
[ADCP -18m; ADCP -26m]
0.5 ms-1
39°N
30'
38°N
30'
37°N
30'
36°N
1°W
0°
1°E
2°E
3°E
4°E
5°E
Latitude
Longitude
0.15
0.1
0.05
0
-0.05
adt (m)

**FIG 14**

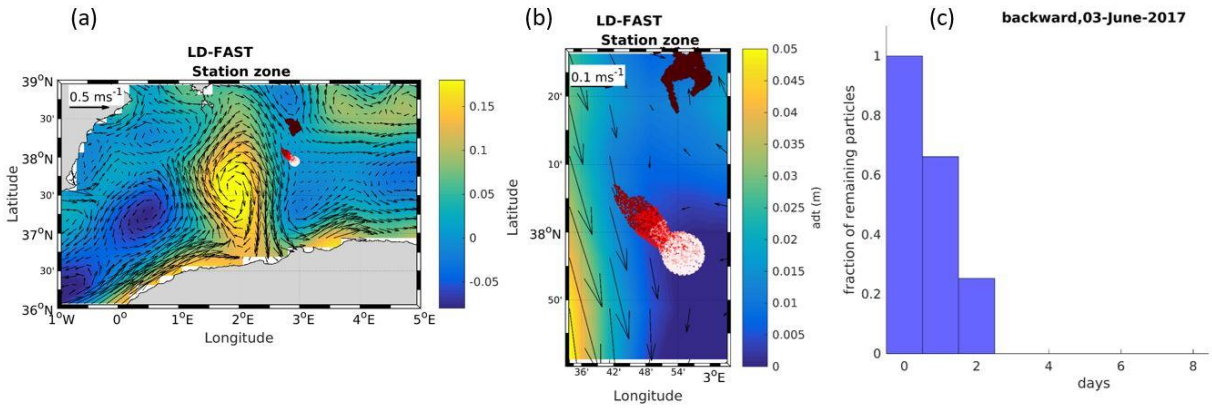
(a)
LD-FAST
Station zone
0.5 ms-1
Latitude
Longitude
(b)
LD-FAST
Station zone
0.1 ms-1
Latitude
Longitude
adt (m)
(c)
backward,03-June-2017
fraction of remaining particles
days

**FIG 15**

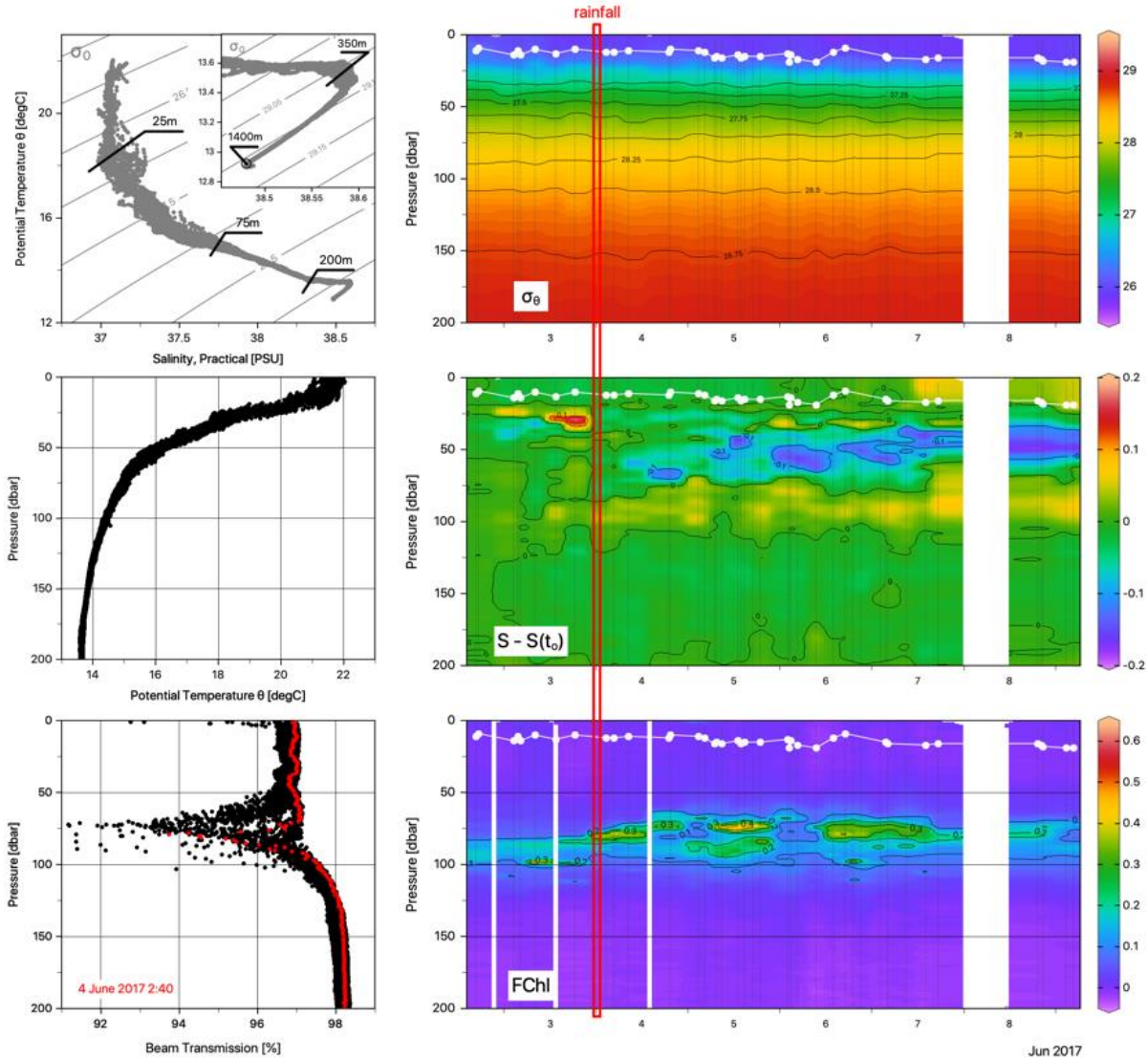
rainfall
Potential Temperature θ [degC]
Salinity, Practical [PSU]
25m
75m
200m
350m
1400m
Pressure [dbar]
Potential Temperature θ [degC]
Beam Transmission [%]
4 June 2017 2:40
σθ
S - S(t0)
FChl
Jun 2017

**FIG 16**

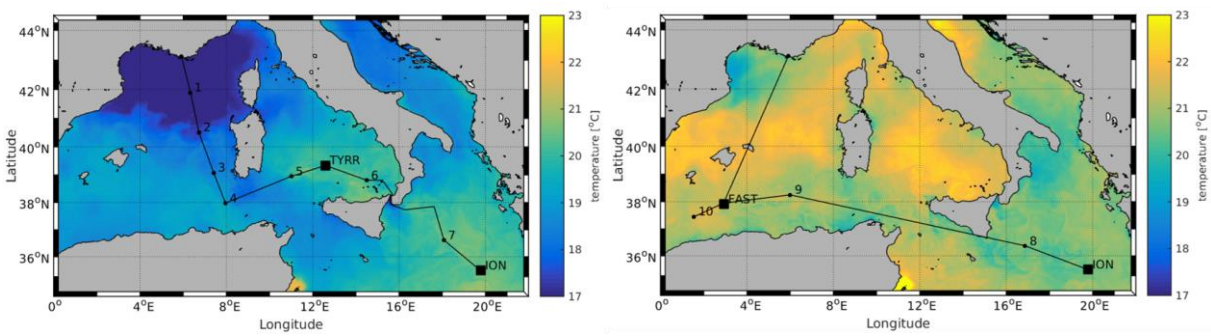
Latitude
Longitude
temperature [°C]
TYRR
ION
EAST

**FIG 17**

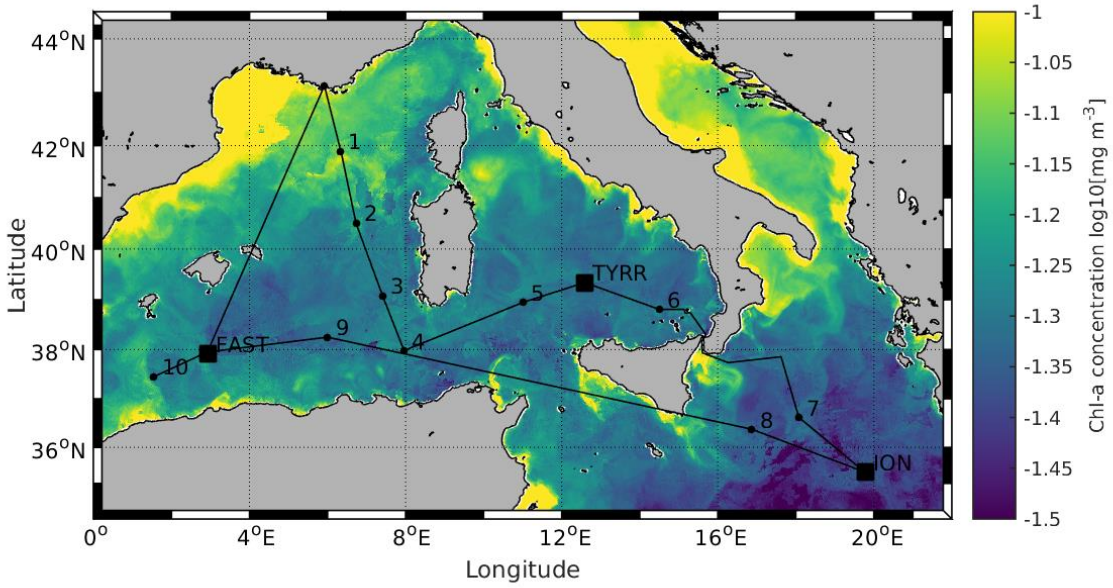
44°N
42°N
40°N
38°N
36°N
Latitude
0°
4°E
8°E
12°E
16°E
20°E
Longitude
1
2
3
4
5
6
7
8
9
10
TYRR
EAST
ION
-1
-1.05
-1.1
-1.15
-1.2
-1.25
-1.3
-1.35
-1.4
-1.45
-1.5
Chl-a concentration log10[mg m-3]

**FIG 18**

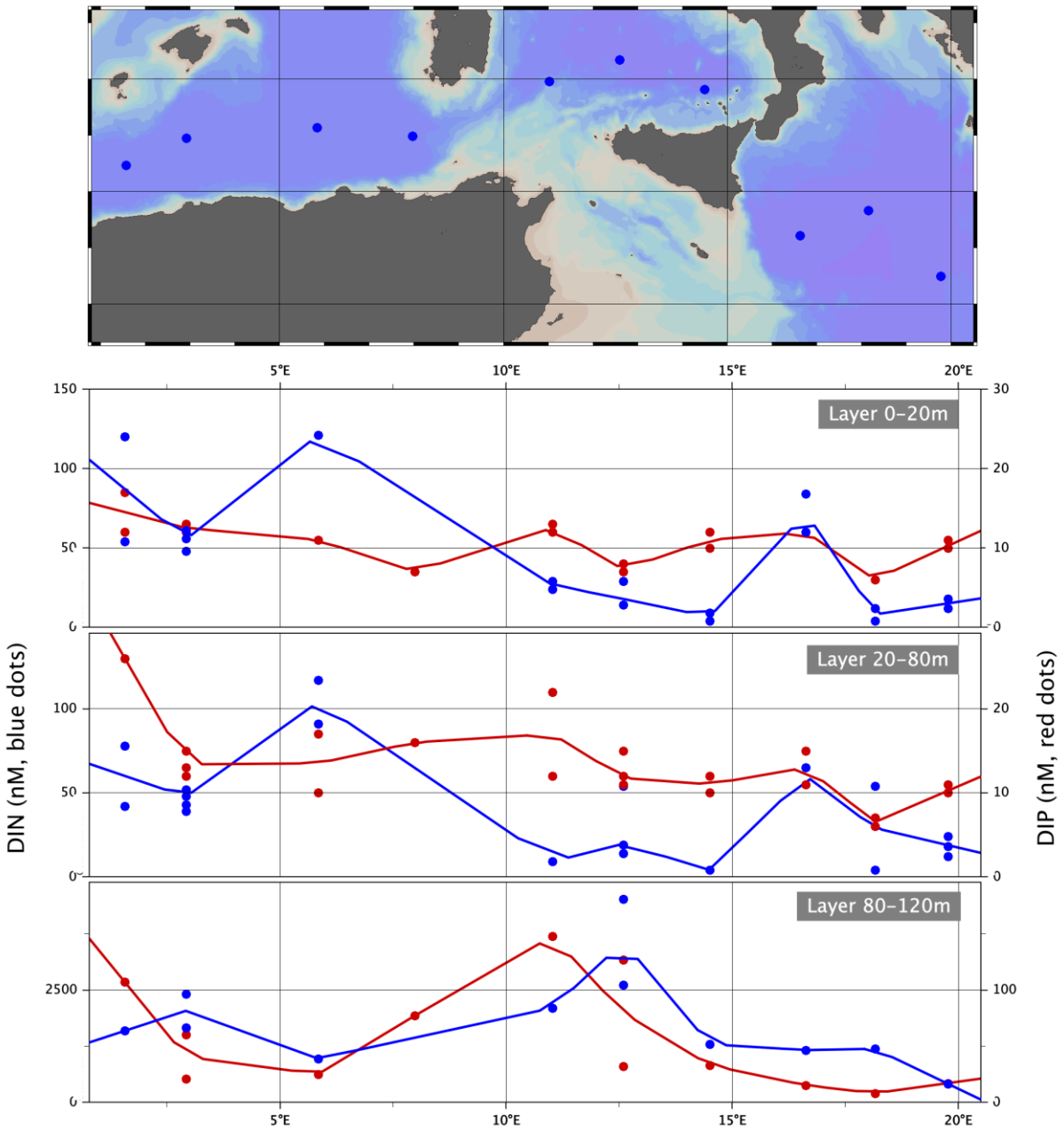
5°E
10°E
15°E
20°E
Layer 0–20m
Layer 20–80m
Layer 80–120m
DIN (nM, blue dots)
DIP (nM, red dots)
150
100
50
0
30
20
10
2500